6mer seed toxicity in tumor suppressive microRNAs

Quan Q. Gao[1,6], William E. Putzbach[1,6], Andrea E. Murmann[1], Siquan Chen[2], Aishe A. Sarshad[3], Johannes M. Peter[4], Elizabeth T. Bartom[5], Markus Hafner[3], and Marcus E. Peter[1,5]

[1]Department of Medicine/Division Hematology/Oncology and [5]Department of Biochemistry and Molecular Genetics, Northwestern University, Chicago, IL 60611, USA, [2]Cellular Screening Center, Institute for Genomics & Systems Biology, The University of Chicago, Chicago, IL 60637, USA, [3]Laboratory of Muscle Stem Cells and Gene Regulation, NIAMS, NIH, Bethesda, MD 20892, USA, [4]DigiPen Institute of Technology, Redmond, WA 98052, USA,

[6] Authors share first authorship

Corresponding author: Marcus E. Peter, E-mail: m-peter@northwestern.edu, phone: 312-503-1291; FAX: 312-503-0189.

Keywords: DISE, RNAi, miRNAs, strand selection, toxicity, evolution

SUMMARY

Many small interfering (si)RNAs are toxic to cancer cells through a 6mer seed sequence (position 2-7 of the guide strand). Here we performed a siRNA screen with all 4096 6mer seeds revealing a preference for guanine in positions 1 and 2 and a high overall G or C content in the seed of the most toxic siRNAs for four tested human and mouse cell lines. Toxicity of these siRNAs stems from targeting survival genes with C-rich 3'UTRs. The master tumor suppressor miRNA miR-34a-5p is toxic through such a G-rich 6mer seed and is upregulated in cells subjected to genotoxic stress. An analysis of all mature miRNAs suggests that during evolution most miRNAs evolved to avoid guanine at the 5' end of the 6mer seed sequence of the guide strand. In contrast, for certain tumor suppressive miRNAs the guide strand contains a G-rich toxic 6mer seed, presumably to eliminate cancer cells.

INTRODUCTION

RNA interference (RNAi) is a form of post-transcriptional regulation exerted by 19-21 nt long double stranded RNAs that negatively regulate gene expression at the mRNA level. RNAi-active guide RNAs can come from endogenous siRNAs and micro(mi)RNAs. For a miRNA, the RNAi pathway begins in the nucleus with transcription of a primary miRNA precursor (pri-miRNA) [1]. Pri-miRNAs are first processed by the Drosha/DGCR8 microprocessor complex into pre-miRNAs [2], which are then exported from the nucleus to the cytoplasm by Exportin 5 [3]. Once in the cytoplasm, Dicer processes them further [4, 5] and these mature dsRNA duplexes are then loaded into Argonaute (Ago) proteins to form the RNA-induced silencing complex (RISC) [6]. The sense/passenger strand is ejected/degraded, while the guide strand remains associated with the RISC [7]. Depending on the degree of complementarity between the guide strand and its target, the outcome of RNAi can either be target degradation - most often achieved by siRNAs with full complementarity to their target mRNA [8] - or miRNA-like cleavage-independent silencing, mediated by deadenylation/degradation or translational repression [9]. The latter mechanism can be initiated with as little as six nucleotide base-pairing between a guide RNA's so-called seed sequence (positions 2 to 7) and fully complementary seed matches in the target RNA [10, 11]. This seed-based targeting most often occurs in the 3'UTR of a target mRNA [12, 13].

A number of miRNAs function either as tumor suppressors or as oncogenes [14]. Their cancer specific activities are usually explained by their identified targets, being oncogenes or tumor suppressors, respectively [14]. Examples of targets of tumor-suppressive miRNAs are the oncogenes Bcl-2 for miR-15/16 [15] and c-Myc for miR-34a [16]. While many miRNAs have been reported to have both tumor suppressive and oncogenic activities depending on the cancer context, examples for widely established tumor promoting miRNAs are miR-221/222, miR-21, miR-155, and members of the miR-17~92 cluster, or its paralogues miR-106b~25 and miR-106a~363 [17, 18]. In contrast, two of the major tumor suppressive miRNA families are miR-15/16 and the p53 regulated miR-34a/c and miR-34b [19].

66 We recently discovered that many si- and shRNAs can kill all tested cancer cell lines through RNAi by
67 targeting the 3'UTRs of critical survival genes [20]. We called this mechanism DISE (for death induced by
68 survival gene elimination). Cancer cells have difficulty developing resistance to this mechanism both *in vitro*
69 and when treated *in vivo* [21]. We reported that a 6mer seed sequence in the toxic siRNAs is sufficient for
70 effective killing [20]. We have now performed a strand specific siRNA screen with a library of individual
71 siRNAs representing all 4096 possible 6mer seed sequences in a neutral RNA duplex. This screen, while
72 based on siRNA biochemistry was not designed to identify targets that are degraded through siRNA
73 mediated slicing activity but to identify toxicity caused by moderately targeting hundreds of genes required
74 for cell survival in a mechanism similar to miRNA-induced silencing.
75 We report that the most toxic 6mer seeds are G-rich with a G enrichment towards the 5' end targeting
76 survival genes with a high C content in their 3'UTR in a miRNA-like manner. Many tumor suppressive
77 miRNAs such as miR-34a-5p but none of the established oncogenic miRNAs contain G-rich 6mer seeds and
78 most of miR-34a-5p's toxicity comes from its 6mer seed sequence. Mature miRNAs from older and more
79 conserved miRNAs contain less toxic seeds. We demonstrate that for most miRNAs the more abundant
80 mature form corresponds to the arm that contains the less toxic seed. In contrast, for major tumor suppressive
81 miRNAs, the mature miRNA is derived from the arm that harbors the more toxic seed. Our data allow us to
82 conclude that while most miRNAs have evolved to avoid targeting survival and housekeeping genes, certain
83 tumor suppressive miRNAs function to kill cancer cells through a toxic G-rich 6mer seed targeting the
84 3'UTR of survival genes.
85
86 **RESULTS**
87 **Identifying the most toxic 6mer seeds**
88 To test whether certain 6mer seeds present in the guide strand of a siRNA affect cancer cell survival, we
89 recently designed a neutral 19mer oligonucleotide scaffold with two nucleotide 3' overhangs, and we
90 demonstrated that modifying a siRNA strand at positions 1 and 2 by 2'-O-methylation (OMe) completely
91 blocks its loading into the RISC [22]. Different 6mer sequences can be inserted at positions 2-7 of the guide
92 strand with the designated passenger strand modified by OMe (two red Xs in **Fig. 1a**). Transfection
93 efficiency and conditions were optimized for each cell line used. To determine the general rules of seed-
94 based toxicity, we individually transfected 4096 siRNAs with all possible 6mer seed sequences in this 19mer
95 scaffold into two human, HeyA8 (ovarian cancer) and H460 (lung cancer), and two mouse cell lines M565
96 (liver cancer) and 3LL (lung cancer). This allowed us to rank all 4096 6mer seeds according to their toxicity
97 (**Fig. 1b**, **Supplementary Data File 1,** and **6merdb.org**). The congruence between the results of the two
98 human cell lines and the two human and two mouse cell lines was quite high (r=0.68 and 0.73, respectively,
99 **Fig. 1c**) suggesting that many siRNAs were toxic through a mechanism independent of cancer origin and

species. Toxicity was caused by the different 6mer seeds in the *guide* strand. A siRNA duplex highly toxic to all cell lines (#2733, HeyA8 cell viability = 1.4%) strongly inhibited cell growth and reduced cell viability of HeyA8 cells only when the passenger strand but not when the guide strand was modified by the OMe modification. Toxicity was completely blocked when the guide strand was modified (**Supplementary Figure 1a**). The toxicity was due to RNAi as knockdown of AGO2 abolished the toxicity of two of the most toxic siRNAs (**Supplementary Figure 1b**).

We previously reported that the CD95 ligand (CD95L) coding region (CDS) is enriched in sequences that when converted into si- or shRNAs are toxic to cancer cells [20] and most recently that the CD95L mRNA itself is toxic to cells [23]. We now report a substantial correlation between the most toxic CD95L-derived shRNAs and the toxicity of their predicted 6mer seed (**Fig. 1d**) suggesting the CD95L-derived si/shRNAs kill cancer cells through 6mer seed toxicity. Consistent with this assumption we found that the 6mer seeds of 4 previously tested siRNAs derived from CD95L [24] in this screen were about as toxic as the full length siRNAs, with $siL3^{Seed}$ being the most toxic followed by $siL2^{Seed}$ and less or no toxicity associated with $siL4^{Seed}$ and $siL1^{Seed}$ (**Fig. 1b, Fig. 1c**). Our recent analysis suggested that the toxic si/shRNAs act like artificial miRNAs by targeting the 3'UTR of mRNAs [20].

6mer seeds enriched in G at the 5'end are most toxic

We noticed that the 6mer seeds in siL3 and siL2 have a higher G content than the ones in siL4 and siL1 (**Fig. 1b**). By analyzing the screen results of all four cell lines (**Supplementary Figure 2**), we found that a high G content of the seed correlated better with toxicity than a high C content. Almost no toxicity was found with seeds with a high A content. To test the effect of nucleotide content on toxicity directly, we retested the 19 seed duplexes with the highest content (>80%) for each of the four nucleotides in the four cell lines (**Fig. 2**). The reanalysis also allowed us to determine the reproducibility of the results obtained in the large screens (which for technical reasons had to be performed in three sets). All data on the three cell lines were highly reproducible especially for the most toxic seeds (**Supplementary Figure 3a**). When the data on the four cell lines were compared, it became apparent that in all cell lines, the G-rich seeds were by far the most toxic followed by the C-rich, U-rich, and A-rich seeds (**Fig. 2a**). This indicates it is mostly the G content that determines toxicity.

Most genome-wide siRNA libraries designed to study functions of individual genes are highly underrepresented in G and C to increase RNAi specificity [25] (**Supplementary Figure 3b**, left panel). In contrast, our complete set of 6mer seed duplexes exhibits no nucleotide composition bias, allowing us to test the contributions of all four nucleotides in each of the 6 seed positions (**Supplementary Figure 3b**, right panel). To determine the nucleotide content of the most toxic seeds, we determined the frequency of each nucleotide at each of the 6 positions of either the 200 most or 200 least toxic seed duplexes for each of the

134 two human and the two mouse cells (**Fig. 2b**, **Supplementary Data File 1**). We found that a high G
135 content towards the 5' end of the seed and a C in position 6 was most toxic (**Fig. 2b** and **Supplementary**
136 **Figure 3c**). In contrast, non-toxic seeds were A and U-rich especially when positioned at the 5' end. The
137 rules of toxicity that emerged are almost identical between human and mouse, suggesting evolutionary
138 conservation. This can also be explored at 6merdb.org.
139

140 **Toxic siRNAs target C-rich housekeeping genes**

141 We previously showed that si- and shRNAs are toxic through 6mer seed toxicity preferentially targeting
142 hundreds of genes critical for cell survival [20]. We had developed a Toxicity Index (TI), a simple tool to
143 predict the most toxic seeds based on the ratio of putative seed match occurrences in the 3'UTR of set of
144 survival genes (SGs) versus a set of genes not required for cell survival (nonSGs). We now compared the TI
145 with our experimentally determined 6mer seed toxicity in the four cell lines screened (**Supplementary**
146 **Figure 4**) and found a significant correlation between these two types of analyses, further supporting the
147 mechanism of toxicity. Knowing that seed sequences rich in G are most toxic suggested the targeted genes
148 carry C-rich seed matches in their 3'UTR. To be most stringent, we used a list of the 20 6mer seeds that were
149 most toxic to both HeyA8 and H460 cells (**Supplementary Data File 2**). The G richness towards the 5' end
150 of the 6mers in these toxic seeds and the 5' A/U richness of the nontoxic seeds was even more pronounced
151 than in the top/bottom 200 most toxic seeds (**Fig. 3a**). We scored for the occurrence of seed matches to the
152 20 seeds in each group in the 3'UTR, the CDS and the 5'UTR of a set of 938 critical SGs similar to one
153 recently described [20] and an expression-matched set of 938 nonSGs. We found a significantly higher count
154 ratio of toxic versus nontoxic seed matches in the 3'UTR of SGs when compared to nonSGs (**Fig. 3b**, right
155 panel). Consistent with a miRNA-like function no such enrichment was found when the CDS was analyzed
156 (**Fig. 3b**, center panel). An inverse ratio of sequences complementary to the 6mer seeds of unknown
157 significance was found in the 5'UTR (**Fig. 3b**, left panel). This result was very similar when we scored for
158 seed matches to the 100 seeds most toxic and least toxic to both human cell lines (**Supplementary Figure**
159 **5a**). An enrichment of the exact seed matches in 3'UTRs was consistent with the overall higher C content of
160 3'UTRs of SGs when compared to nonSGs (different peak maxima in **Fig. 3c**). A metaplot analysis of the
161 500 bases upstream and downstream of the translational start and stop site of all human genes showed that as
162 expected the 3'UTR was enriched in A and U (**Fig. 3d**, top). Interestingly, SGs had a lower A/U content in a
163 region ~150-500 bases into the 3'UTR than expression matched nonSGs (**Fig. 3d**, blue horizontal bar, bottom
164 two panels). To determine where survival genes are being targeted by toxic seed containing siRNAs we
165 again performed a metaplot analysis - this time plotting the locations of seed matches to the 20 6mer seeds
166 that were most and least toxic to both human cell lines (**Fig. 3e**, an analysis with the 100 most/least toxic
167 seeds is provided in **Supplementary Figure 5b**). When analyzing all human coding genes we found the

168 reverse complements of the most toxic seeds to be highly enriched at the beginning of the 3'UTR whereas
169 the reverse complements of the least toxic seeds were underrepresented in this region (**Fig. 3e**, top). This
170 effect was not due to a much higher G/C or lower A/U content in this region (**Fig. 3d**, top). A comparison of
171 the location of these seed matches in the SGs and in expression matched nonSGs confirmed this general
172 trend, however, two differences between SGs and nonSGs became apparent: 1) nonSGs have more nontoxic
173 seed matches ~150-500 bases into the 3'UTR (**Fig. 3e**, bottom, blue horizontal bar) maybe due to the higher
174 A/U content of this region (**Fig. 3d**, two bottom panels). 2) SGs contain a small stretch at positions 42-65
175 into the 3'UTR (**Fig. 3e** and **Supplementary Figure 5b**, center, green horizontal bar) that is enriched in seed
176 matches for the most toxic seeds. This region in SGs seems to be a preferential target site for siRNAs
177 carrying toxic G-rich seed sequences.
178

179 **miR-34a-5p kills cancer cells through its toxic 6mer seed**

180 The toxic siRNAs kill cancer cells through 6mer seed toxicity by a mechanism reminiscent of the function of
181 miRNAs. To test whether actual miRNAs could kill cancer cells with the help of toxic 6mer seeds, we
182 analyzed the seed toxicity determined in our screen for all known ~2600 mature miRNAs expressed as either
183 the 3p or 5p arm (**6merdb.org**). While none of the 6mer seeds present in the predominant arm (guide strand)
184 of the most oncogenic miRNAs (miR-221/222, miR-21, miR-155, the miR-17~92, miR-106b~25, and miR-
185 106a~36 clusters) were toxic (reduced viability >50%, stippled line in **Fig. 4a**), two of the major tumor
186 suppressive miRNA families, miR-15/16 and p53 regulated miR-34a/c and miR-34b contained toxic seeds in
187 the guide strand (**Fig. 4a**). This suggested these two families were killing cancer cells through toxic 6mer
188 seeds. Interestingly, two other major tumor suppressive families, let-7 and miR-200, did not contain toxic G-
189 rich seeds in their guide strand, suggesting they may be tumor suppressive through other mechanisms, such
190 as inducing and maintaining cell differentiation [26].

191 When transfecting the pre-miRs of miR-34a-5p, miR-15a-5p, and let-7a-5p into HeyA8 cells, the potency
192 of these three miRNAs to reduce cell growth mimicked the toxicity of their 6mer seed containing siRNAs
193 (**Fig. 4b** and **4a**). This suggested that a large part of their toxicity comes from the composition of the seed
194 position 2-7. The most toxic seed in a major tumor suppressive miRNA was present in miR-34a-5p/34c-5p, a
195 master regulator of tumor suppression [27]. We directly compared the toxicity of pre-miR-34a-5p and its toxic
196 seed in the neutral scaffold with blocked passenger strand (si34a-5p^{Seed}) in the same assays (**Fig. 4c**).
197 Strikingly, the toxicity evoked by these two RNA species (assessed by growth inhibition and DNA
198 fragmentation) was similar. Cells showed the typical morphology we found in cells dying from toxic siRNAs
199 (**Fig. 4d**) [20, 24, 28]. To determine the contribution of the 6mer seed sequence of miR-34a-5p to its toxicity and
200 the mode of cell death, we performed a RNA-Seq analysis on HeyA8 cells transfected with either miR-34a-
201 5p or si34a-5p^{Seed} (**Fig. 5a**, top) (**Supplementary Data File 3**). The vast majority of genes were significantly

202 up- and downregulated by both RNA duplexes (**Fig. 5a**, bottom). While miR-34a-5p targeted a subset of
203 genes not affected by miR-34a-5p^{Seed}, the majority of differentially expressed genes (>78%) were
204 downregulated >1.5 fold by both the premiR and the 6mer seed duplex (**Fig. 5b**, left). A Sylamer analysis is
205 a unbiased approach allowing to identify which seed matches are enriched in the 3'UTRs of downregulated
206 genes from RNAseq data [29]. In this analysis both duplexes caused similar and highly effective
207 downregulation of the mRNAs that carry a 6mer seed match (**Fig. 5c**). When the Sylamer analysis was
208 performed with either 7mer or 8mer seeds, enrichment of seed matches was much less significant
209 (**Supplementary Figure 6a**) suggesting that most of the targeting by both RNAs only required a 6mer seed.
210 Consistent with this activity, targeting by both RNA duplexes resulted in a very similar reduction of
211 survival genes (**Fig. 5d**). The genes downregulated by both the premiR and the 6mer seed construct were
212 highly enriched in genes involved in regulation of cell cycle, cell division, DNA repair, and nucleosome
213 assembly (**Fig. 5b**, right). These GO terms were very similar to the ones we found enriched in downregulated
214 genes in cells dying after transfection with CD95R/L-derived si/shRNAs containing toxic 6mer seeds [20]. In
215 contrast, no such GO terms were found enriched when the same analysis was performed with the upregulated
216 genes as control (**Supplementary Figure 6b**). While both miR-34-5p and si34a-5p^{Seed} caused the most
217 significant downregulation of genes carrying 8mers in their 3'UTR (**Supplementary Figure 6c**), only the
218 most highly downregulated genes that carry the shared 6mer seed match were grouped in a number of GO
219 terms that are consistent with 6mer seed toxicity as previously reported [20] and barely any GO terms were
220 shared among genes that contained 7 or 8mer seed matches (**Supplementary Figure 6d**). All these data
221 suggest that miR-34a-5p kills cancer cells using its toxic 6mer seed. While optimal miRNA targeting
222 requires at least a 7mer seed interaction and also involves nucleotides at positions 13-16 of the miRNA [30],
223 the cell death inducing activity of this tumor suppressive miRNA may only require the 6mer seed.
224

225 **Toxic 6mer seed toxicity is shaping the miRNA repertoire**

226 Toxic 6mer seeds may be a driving force in miRNA evolution, whereby toxic seed sequences are either
227 selected against - because they contribute to cell toxicity - or are preserved to operate as tumor suppressors.
228 Based on the composition of toxic 6mer seeds and the enrichment of corresponding seed matches in survival
229 genes, we could now ask whether and when miRNAs that contain toxic G-rich sequences in positions 2-7 of
230 their seeds evolved. When comparing all mature miRNA arms annotated in TargetScan Human 7, we noticed
231 that miRNAs in highly conserved miRNA seed families contained 6mer seed sequences that were much less
232 toxic in our screen than seeds in poorly conserved miRNAs (**Fig. 6a,** left panel and **Supplementary Figure**
233 **7a**). Weakly conserved miRNA seed families would be expected to be younger in evolutionary age than
234 highly conserved ones. Consistent with this assumption we found that the 6mer seeds of younger miRNAs
235 (<10 million years old) were more likely to be toxic to cells than the ones of older miRNAs (>800 million

236 years old) [31] (**Fig. 6a**, right panel and **Supplementary Figure 7b**). Most importantly, when comparing
237 miRNAs of different ages, it became apparent that seeds of miRNAs over the last 800 million years were
238 gradually depleted of G beginning at the 5' end and eventually also affecting positions 3-5 until the oldest
239 ones, where A and U had replaced G as the most abundant nucleotide in all six positions (**Fig. 6b**). These
240 analyses indicated that most highly conserved miRNAs avoid G in potentially toxic seed positions.
241 Interestingly, the most toxic seed sequences were found in miRtrons (**Fig. 6c** and **Supplementary Figure**
242 **7c**), miRNAs that are derived by splicing short introns [32]. Across all mature miRtrons we found G to be the
243 most abundant nucleotide in position 2-7 (**Supplementary Figure 7d**) and this region was also near the
244 region in all miRtrons predicted to contain the 6mer sequences with the highest toxicity (**Supplementary**
245 **Figure 7e**).

246 miRNAs are expressed as pre-miRs and usually only one major species of mature miRNA (either the 5p
247 or the 3p arm) is significantly expressed in cells produced from one of the two strands of the premiR stem [33].
248 Consistent with the assumption that cells cannot tolerate toxic 6mer seeds, we now examined across 780
249 miRNAs which have been shown to give rise to both a 3p and a 5p arm whether the more highly expressed
250 arm contains a seed of lower toxicity than the lesser expressed arm (**Fig. 6d**). We ranked the miRNAs
251 according to the ratio of the 6mer seed toxicity associated with the guide arm to the lesser-expressed arm
252 (**Supplementary Data File 4**). When we labeled the major tumor suppressive and oncogenic miRNAs, we
253 noticed the highly expressed arm of most of the oncogenic miRNAs contained a 6mer seed that was not toxic
254 in our screen (**Fig. 6d**, blue dots). In contrast, for most of the tumor suppressive miRNAs, the dominant arm
255 contained a seed much more toxic than the lesser arm (**Fig. 6d**, red dots). The overall difference in ratio
256 between the two groups of miRNAs was highly significant. A more detailed analysis of these data revealed
257 that the three oncogenic miRNAs with the highest ratio in toxicity between their arms, miR-363, miR-92a-2,
258 and miR-25, were almost exclusively expressed as the non-toxic 3p form (**Fig. 6e**, top). In contrast, the
259 dominant arm of the three tumor suppressive miRNAs, miR-34a, miR-34c, and miR-449b contained the most
260 toxic seed sequence (**Fig. 6e**, bottom). Interestingly, miR-449b has the same seed sequence as miR-34a and
261 has been suggested to act as a backup miRNA for miR-34a [34]. These data are consistent with most tumor
262 suppressive miRNAs using 6mer seed toxicity to kill cancer cells and suggest that this mechanism developed
263 over hundreds of millions of years.
264

265 **Genotoxic drugs upregulate toxic 6mer seed containing miRNAs**

266 Our data showing that miR-34a-5p contains a toxic 6mer seed, along with miR-34a being upregulated after
267 genotoxic stress [19], led us to wonder whether miR-34a-5p would contribute to cell death induced by
268 genotoxic drugs and whether this type of cell death shared similarities to the death observed in cells dying
269 from toxic 6mer seed containing si/shRNAs. This would be consistent with the observation that many

270 genotoxic drugs induce multiple cell death pathways [35, 36, 37, 38, 39]. To compare cell death induced by
271 different genotoxic agents with that of toxic si/shRNAs, we treated the p53 wild-type ovarian cancer cell line
272 HeyA8 with doxorubicin (Doxo), carboplatin (Carbo), or etoposide (Eto) and performed a RNA-Seq
273 analysis. Drug concentrations were chosen so that after 80 hrs, treatment would slow down cell growth and
274 induce signs of stress without major cell death occurring to capture changes that could be causing cell death
275 rather than being the result of it (**Supplementary Figure 8a**). The morphological changes in the cells treated
276 with the drugs were very similar to the ones seen in cells treated with si/shRNAs (**Supplementary Figure**
277 **8b**), and similar to reported morphologies of cells treated with genotoxic drugs [40, 41].

278 The ranked lists of downregulated RNAs isolated from HeyA8 cells treated with the three drugs were
279 subjected to a gene set enrichment analysis (GSEA) to determine whether survival genes were enriched in
280 the downregulated genes (**Supplementary Figure 9a**). There was strong enrichment of downregulated
281 survival genes towards the top of the ranked list. 102 of the survival genes were downregulated in cells
282 treated with any of the three drugs (**Supplementary Figure 9b**). In a DAVID gene ontology analysis, these
283 genes were strongly enriched in clusters involved in chromosome segregation, DNA replication, cell cycle
284 regulation, and mitosis, typical for 6mer seed toxicity induced cell death (**Supplementary Data File 5**). We
285 quantified 30 of the 102 survival genes in HeyA8 cells treated with Doxo at different time points using an
286 arrayed quantitative PCR (**Supplementary Figure 9c**). 24 of the 30 genes' mRNAs were significantly
287 downregulated as early as 7 hours after treatment with no further reduction beyond 15 hrs after treatment,
288 suggesting that their repression was the cause of cell death rather than a consequence. A Metascape analysis
289 of all RNA-Seq data of downregulated RNAs in response to the toxic siL3, si34a-5p^{Seed}, miR-34a-5p, and the
290 three genotoxic drugs suggested a common mode of action (**Supplementary Figure 9d**). The GO clusters
291 that were most significantly downregulated in all data sets were again related to DNA repair, cell cycle, and
292 mitosis as described before for cells undergoing DISE [24].

293 To test whether treatment of cells with genotoxic drugs results in loading the RISC with toxic miRNAs,
294 HeyA8 cells were treated with Doxo for 0, 20, 40 and 80 hrs and all 4 Ago proteins were pulled down using
295 a GW182 peptide [42]. Interestingly, while the amount of AGO2 pulled down was the same at all time points,
296 the amount of bound miRNA-sized RNAs substantially increased with longer treatment times (**Fig. 7a**). This
297 was most likely the result of an overall increase in total small RNAs in the treated cells (**Fig. 7b**).
298 Alternatively, this could also be a result of cells dividing more slowly and a stable RISC. miR-34a/b/c-5p
299 bound to Ago proteins were upregulated at all time points (**Supplementary Figure 10a**). To determine the
300 contribution of miR-34a-5p and other miRNAs to the toxicity seen in cells exposed to the genotoxic drugs,
301 we treated *Drosha* k.o. cells - devoid of most canonical miRNAs [43] - with the three genotoxic drugs
302 (**Supplementary Figure 11a**). These cells were hypersensitive to the toxicity induced by any of the three
303 drugs. We attributed this response to the absence of most canonical miRNAs that protect cells from toxic

304 RNAi active sequences [20]. This result also suggested involvement of small RNAs that do not require
305 Drosha for processing. As expected, the composition of small RNAs bound to Ago proteins dramatically
306 varied between wild-type and *Drosha* k.o. cells (**Fig. 7c**). In the absence of most canonical miRNAs, miR-
307 320a-3p, which was previously shown not to require Drosha for its biogenesis [43], represented more than 86%
308 of all Ago-bound miRNAs. Similar to HeyA8 cells (see **Supplementary Figure 10a**), Ago-bound miR-34a-
309 5p was upregulated in wild-type but not in *Drosha* k.o. HCT116 cells upon Doxo treatment (**Supplementary**
310 **Figure 10b**, right). Interestingly, the average 6mer seed toxicity of all Ago-bound miRNAs >1.5 fold
311 upregulated in HCT116 wt cells was significantly higher than the ones >1.5 fold downregulated in cells
312 treated with Doxo (**Fig. 7d**, left). While in the *Drosha* k.o. cells, a number of nontoxic miRNAs were
313 downregulated, the only miRNA that was upregulated in the RISC (1.49 fold) was miR-320a-3p (**Fig. 7d**,
314 right). However, upon closer inspection it became clear that this form of miR-320a-3p was shortened by two
315 nucleotides at the 5' end. This resulted in the shift of the 6mer seed into a G-rich sequence (**Fig. 7d**, right),
316 converting a moderately toxic miRNA (average viability = 49.2%) into a highly toxic one (average viability
317 = 9.3%). To test this predicted increase in toxicity experimentally, we transfected HeyA8 cells with either the
318 authentic pre-miR-320a-3p or a miR-320a-3p^{Seed} duplex that corresponded to the shifted Ago-bound miR-
319 320a-3p sequence (miR-320a-3p^{Ago}) (**Fig. 7e**). While pre-miR-320a-3p was not toxic, miR-320a-3p^{Ago}
320 completely blocked the growth of the cells. Toxicity of miR-320a-3p^{Ago} was established in the four human
321 and mouse cell lines (**Fig. 7f**). These data suggested that in the absence of other miRNAs that could kill cells
322 through 6mer seed toxicity, miR-320a-3p (and possibly other small RNAs) may represent an alternative
323 mechanism that ensures that genotoxic stressors can kill cells with defective miRNA processing often
324 observed in cancer [44, 45]. To test whether the 6mer seed toxicity exerted by miR-34a would be synergistic
325 with the toxicity caused by the three genotoxic drugs, we treated HeyA8 cells with a low dose (1 nM) of
326 miR-34a with low doses of either Doxo, Eto or Carbo (**Supplementary Figure 11b**). No synergism was
327 observed consistent with the assumption that genotoxic drugs are killing the cells at least in part through the
328 use of toxic RNAi active RNAs. In summary, our data suggest that certain tumor suppressive miRNAs, such
329 as miR-34a-5p and miR-320a-3p exert their tumor suppressive activities by carrying toxic 6mer seed
330 sequences that can kill cancer cells by targeting survival genes in C-rich regions close to the start of their
331 3'UTR. This activity may contribute to the cell death induced by genotoxic drugs.
332

333 **DISCUSSION**

334

335 We previously discovered a fundamental cell type- and species-independent form of toxicity that is evoked
336 by the 6mer seed sequence in si-/shRNAs that function similar to miRNAs [20]. We have now performed an
337 siRNA screen that effectively tested the miRNA activities of all 4096 different 6mer seed sequences.

338 Performing the screen in four cell lines (two human and two mouse) ensured that the results were
339 relatively independent of species or cell type specific transcriptomes. The screen has discovered the rules
340 underlying this seed toxicity and allows prediction of the 6mer seed toxicity for any siRNA, shRNA, miRNA
341 with a known 6mer seed (https://6merdb.org).

342 Based on this screen, the toxicity of a number of tumor suppressive miRNAs could be predicted solely
343 on the basis of their 6mer seed sequences. The enrichment of G in the first 2-3 positions of the most toxic
344 seeds is consistent with the way Ago proteins scan mRNAs as targets. This involves mainly the first few
345 nucleotides (positions 1-3) of the seed [46]. miR-34a-5p contains two Gs in positions 1 and 2 of its 6mer seed.
346 While miR-34a-5p is considered a master tumor suppressive miRNA, no single target has been identified to
347 be responsible for this activity. Over 700 targets implicated in cancer cell proliferation, survival, and
348 resistance to therapy have been described [16]. Our data now suggest that miR-34a-5p uses 6mer seed toxicity
349 to target hundreds of housekeeping genes. They provide the means to rationally design new artificial
350 miRNAs as anti-cancer reagents that attack networks of survival genes. In humans, miR-34a is highly
351 expressed in many tissues. Consistent with our data that delivering siRNAs with toxic 6mer seeds to mice are
352 not toxic to normal cells [21] miR-34a exhibits low toxicity to normal cells *in vitro* and *in vivo* [47]. miR-34a
353 (MRX34) became the first miRNA to be tested in a phase I clinical trial of unresectable primary liver cancer
354 [27, 48]. The study was recently terminated and reported immune-related adverse effects in several individuals.
355 It was suggested that these adverse effects may have been caused by either a reaction to the liposome-based
356 carrier or the use of double-stranded RNA [16]. In addition, they may be due to an undesired gene modulation
357 by miR-34a itself defined by sequences outside the 6mer seed [16]. Our data suggest that miR-34a exerts
358 toxicity mostly through the 6mer seed of its 5p arm and that its 700 known targets may be part of the
359 network of survival genes that are targeted. The comparison of the RNA-Seq data of cells treated with either
360 miR-34a-5p or si34-5p^{Seed} now allows to determine whether these two activities can be separated.

361 Our data provide evidence that genotoxic drugs kill cancer cells, at least in part, by triggering the toxic
362 6mer seed mechanism. Exposure of cancer cells to such drugs resulted in upregulation of tumor suppressive
363 miRNAs, most prominently of the p53 regulated miR-34 family [19]. While one report demonstrated that
364 inhibiting miR-34a rendered cancer cells more resistant to cell death induced by genotoxic stress [49], another
365 one found no effect of knocking out miR-34a on the sensitivity of HCT116 or MCF-7 cells to Doxo [50]. This
366 mechanism may be highly redundant and may involve many miRNAs. Our analysis of Ago-bound miRNAs
367 in *Drosha* k.o. cells suggest that in the absence of miR-34a, the noncanonical miR-320a-3p which was
368 recently also found to be p53 regulated [51] may act as a backup miRNA that can still respond to genotoxic
369 stress in case the amounts of other miRNAs are reduced, for instance in cases of mutations in miRNA
370 biogenesis associated genes frequently found in human cancers [44]. In addition, recent data suggest that other

371 toxic small RNAs can also be taken up by the RISC and negatively regulate cell growth through their
372 toxic 6mer seed [23].

373 It was shown before that miRNAs overall avoid seed sequences that target the 3‘UTR of
374 survival/housekeeping genes [52, 53]. Survival genes therefore are depleted in seed matches for the most
375 abundant miRNAs in a cell. That also means 3‘UTRs of survival genes must be enriched in sequences not
376 targeted by the seeds present in most miRNAs. Our combined data now suggest it is these sequences that
377 toxic siRNAs and tumor suppressive miRNAs with toxic 6mer seeds are targeting. Our analyses also suggest
378 that most miRNAs have evolved over the last 800 million years by gradually depleting G in their seeds
379 beginning at the 5' end. In addition, the most abundant miRNAs have evolved to use the arm with the lower
380 6mer seed toxicity as the active guide strand, presumably to avoid killing cells. Only in a minority of tumor-
381 suppressive miRNAs does the dominant guide strand contain a toxic seed. By ranking miRNAs according to
382 whether they express the arm with the seed of higher toxicity, it is now possible to identify novel tumor
383 suppressive miRNAs (see 6merdb.org).

384 In summary, we have determined the rules of RNAi targeting by toxic 6mer seeds. These rules allowed
385 us to predict with some confidence which si/shRNAs or miRNAs have the potential to kill cells through their
386 toxic 6mer seed. Toxic miRNAs seem to be involved in killing cancer cells in response to genotoxic drugs.
387 Toxic 6mer seeds are present in a number of tumor-suppressive miRNAs that can kill cancer cells. Our data
388 allow new insights into the evolution of miRNAs and provide evidence that 6mer seed toxicity is shaping the
389 miRNA repertoire. In addition, they now allow to develop super toxic artificial miRNAs for the treatment of
390 cancer.

391

392 **METHODS**

393 **Reagents, cell lines and antibodies**

394 HeyA8 (RRID:CVCL_8878) and H460 (ATCC HTB-177) cells were cultured in RPMI1640 medium
395 (Cellgro Cat#10-040) supplemented with 10% FBS (Sigma Cat#14009C) and 1% L-Glutamine (Corning
396 Cat#25-005). 3LL cells (RRID:CVCL_5653) were cultured in DMEM medium (Gibco Cat#12430054)
397 supplemented with 10% FBS and 1% L-Glutamine. Mouse hepatocellular carcinoma cells M565 were from a
398 spontaneous formed liver cancer in a male mouse carrying a floxed Fas allele [54] and cultured in DMEM/F12
399 (Gibco Cat#11330) supplemented with 10% FBS, 1% L-Glutamine and ITS (Corning #25-800-CR).
400 HCT116 parental (Cat#HC19023, RRID:CVCL_0291) and the *Drosha* k.o. clone (clone #40, Cat#HC19020)
401 were purchased from Korean Collection for Type Cultures (KCTC). Both HCT116 cell lines were cultured in
402 McCoy's 5A medium (ATCC, Cat#30-2007) supplemented with 10% FBS and 1% L-Glutamine. All cell
403 lines were authenticated by STR profiling. Anti-Argonaute-2 antibody (cat#ab186733, 1:1200) was
404 purchased from Abcam, anti-β-actin antibody from Santa Cruz (#sc-47778, 1:5000), and secondary antibody

405 for Western blot was Goat anti-rabbit, IgG-HRP from Southern Biotech (#SB-4030-05, 1:5000).
406 Etoposide (Cat#BML-GR307-0100) was purchased from Enzo Life Sciences, propidium iodide (#P4864)
407 doxorubicin (Cat#D1515) and carboplatin (Cat#C2538) were from Sigma-Aldrich.
408

409 **siRNA screens and cell viability assay**

410 To design the non-toxic siRNA backbone used in the 4096 screen, the siNT2 sequence was used as a starting
411 point and four positions in the center of siNT2 were replaced with the complementary nucleotides in order to
412 remove any identity between the backbone siRNA and the toxic siL3 while retaining the same GC content.
413 Two 2'-O-methylation groups were added to positions 1 and 2 of the passenger strand to prevent loading into
414 the RISC. The 6mer seed region (position 2-7 on the guide strand) was then replaced with one of the 4096
415 possible seeds. Transfection efficiency was optimized for each of the four cell lines individually. RNA
416 duplexes were first diluted with Opti-MEM to make 30 µl solution of 10 nM as final concentration in a
417 384‑well plate by Multidrop Combi. Lipofectamine RNAiMAX (Invitrogen) was diluted in Opti-MEM (6
418 µl lipid + 994 µl of Opti-MEM for HeyA8, 15.2 µl lipid + 984.8 µl of Opti-MEM for M565, 9.3 µl of lipid +
419 990.7 µl of Opti-MEM for 3LL, and 7.3 µl of lipid + 993.7 µl of Opti-MEM for H460). After incubating at
420 room temperature for 5‑10 min, 30 µl of the diluted lipid was dispensed into each well of the plate that
421 contains RNA duplexes. The mixture was pipetted up and down three times by PerkinElmer EP3, incubated
422 at room temperature for at least 20 min, and then, the mixture was mixed again by PerkinElmer EP3. 15 µl of
423 the mixture was then transferred into wells of three new plates (triplicates) using the PerkinElmer EP3. 50 µl
424 cell suspension containing 320 HeyA8 or 820 M565 or 150 3LL or 420 H460 cells was then added to each
425 well containing the duplex and lipid mix, which results in a final volume of 65 µl. Plates were left at room
426 temperature for 30 min and then moved to a 37°C incubator. 96 hours post transfection, cell viability was
427 assayed using CellTiter‑Glo (Promega) quantifying cellular ATP content. 35 µl medium was removed from
428 each well, and 30 µl CellTiter‑Glo cell viability reagent was added. The plates were shaken for 5 min and
429 incubated at room temperature for 15 min. Luminescence was then read on the BioTek Synergy Neo2. The
430 4096 6mer seed containing duplexes were screened in three sets for each cell line. Each set was comprised of
431 five 384 well plates. A number of control siRNAs of known toxicity (including siNT1 and siL3) was added
432 to each plate to compare reproducibility. All samples were set up in triplicate (on three different plates = 15
433 plates/set). The data in the HeyA8, H460 and M565 screens were normalized to lipid only on each plate. The
434 3LL screen which showed some drift between the sets was normalized to the average viability of the cells to
435 siNT1 correcting the variability between sets.
436

437 **Transfection with short oligonucleotides**

438 For IncuCyte experiments, HeyA8 cells were plated in 50 µl antibiotic free medium in a 96 well plate at
439 1000 cells/well, and 50 µl transfection mix with 0.1 µl RNAiMAX and siRNAs or miRNA precursors were
440 added during the plating. For the AGO2 knockdown experiment, 100,000 cells/well HeyA8 cells were
441 reverse-transfected in six-well plates with either non-targeting (Dharmacon, cat#D-001810-10-05) or an
442 AGO2 targeting siRNA SMARTpool (Dharmacon, cat#L004639-00- 005) at 25 nM. 1 µl RNAiMAX per
443 well was used for HeyA8 cells. Twenty-four hours after transfection with the SMARTpools, cells were
444 reversed-transfected in a 96-well plate with siNT2, si2733, or si2733 (see **Supplementary Data File 1**) at 10
445 nM and monitored in the IncuCyte Zoom. To measure the knockdown efficiency, cells were lysed in RIPA
446 buffer for western blot analysis 48 hours after transfection with the SMARTpools.
447 All custom siRNA oligonucleotides were ordered from integrated DNA technologies (IDT) and annealed
448 according to the manufacturer's instructions. In addition to the 4096 siRNAs of the screen the following
449 siRNA sequences were used:
450 siNT1 sense: rUrGrGrUrUrUrArCrArUrGrUrCrGrArCrUrArATT;
451 siNT1 antisense: rUrUrArGrUrCrGrArCrArUrGrUrArArArCrCrAAA;
452 siNT2 sense: rUrGrGrUrUrUrArCrArUrGrUrUrGrUrGrUrGrATT;
453 siNT2 antisense: rUrCrArCrArCrArArArCrArUrGrUrArArArCrCrAAA;
454 siL3 sense: rGrCrCrCrUrUrCrArArUrUrArCrCrCrArUrArUTT;
455 siL3 antisense: rArUrArUrGrGrGrUrArArUrUrGrArArGrGrGrCAA;
456 si-miR-34a-5p^{Seed} sense: mUmGrGrUrUrUrArCrArUrGrUrArCrUrGrCrCrATT;
457 si-miR-34a-5p^{Seed} antisense: rUrGrGrCrArGrUrArCrArUrGrUrArArArCrCrAAA;
458 miR-320a-3p^{Ago} sense: mCmGrCrCrCrUrCrUrCrArArCrCrCrArGrCrUrUTT
459 miR-320a-3p^{Ago} antisense: rArArGrCrUrGrGrGrUrUrGrArGrArGrGrGrCrGAA.
460 The following miRNA precursors and negative controls were used: hsa-miR-34a-5p (Ambion, Cat. No#
461 PM11030), hsa-let-7a-5p (Ambion, Cat. No# PM10050), hsa-miR-320a-3p (Ambion, Cat. No# PM11621),
462 hsa-miR-15a-5p (Ambion, Cat. No# PM10235), and miRNA precursor negative control #1 (Ambion, Cat.
463 No# AM17110).
464

465 **Western blot analysis**

466 Protein extracts were collected by lysing cells with RIPA lysis buffer (1% SDS, 1% Triton X-100, 1%
467 deoxycholic acid). Protein concentration was quantified using the DC Protein Assay kit (Bio-Rad, Hercules,
468 CA). 30 µg of protein were resolved on 8–12% SDS-PAGE gels and transferred to nitrocellulose membranes
469 (Protran, Whatman) overnight at 25 mA. Membranes were incubated with blocking buffer (5% non-fat milk
470 in 0.1% TBS/Tween-20) for 1 hr at room temperature. Membranes were then incubated with the primary
471 antibody diluted in blocking buffer over night at 4°C. Membranes were washed 3 times with 0.1%

472 TBS/Tween-20. Secondary antibodies were diluted in blocking buffer and applied to membranes for 1 hr
473 at room temperature. After 3 more additional washes, detection was performed using the ECL reagent
474 (Amersham Pharmacia Biotech) and visualized with the chemiluminescence imager G:BOX Chemi XT4
475 (Synoptics). All uncropped Western blots are shown in **Supplementary Figure 12**.
476

477 **Monitoring cell growth by IncuCyte and cell death assays**

478 Cells were seeded between 1000 and 3000 per well in a 96-well plate in triplicates. The plate was then
479 scanned using the IncuCyte ZOOM live-cell imaging system (Essen BioScience). Images were captured
480 every four hours using a 10× objective. Cell confluence was calculated using the IncuCyte ZOOM software
481 (version 2015A). For treatment with genotoxic drugs HeyA8 cells were seeded at 750 cells/well and
482 HCT116 cells were seeded at 3000 cells/well in 96-well plate and treated with one of the three genotoxic
483 drugs (carboplatin, doxorubicin, or etoposide) at various concentrations at the time of plating. Solvent treated
484 (0.025% DMSO in medium) cells were used as control for etoposide. Medium treated cells were used as
485 control for carboplatin and doxorubicin. To assess cell viability, treated cells were subjected to a
486 quantification of nuclear fragmentation or ATP content. To measure the level of nuclear fragmentation, cell
487 pellet (500,000 cells) was resuspended in 0.1% sodium citrate, pH 7.4, 0.05% Triton X-100, and 50 μg/ml
488 propidium iodide. After resuspension, cells were incubated 2 to 4 hrs in the dark at 4°C. The percent of
489 subG1 nuclei (fragmented DNA) was determined by flow cytometry. To measure the cellular ATP content,
490 cells were reverse transfected with siRNAs in a 96 well plate at 1000 cells per well. 96 hours after
491 transfection, media in each well was replaced with 70 µl of fresh media and 70 µl of CellTiter - Glo cell
492 viability reagent (Promega). The plates were shaken for 5 min and incubated at room temperature for 15 min.
493 Luminescence was then read on the BioTek Cytation 5.
494

495 **RNA-Seq analysis**

496 For RNA-Seq data in **Fig. 5a**, 50,000 cells/well HeyA8 cells were reversed transfected in duplicate in 6-well
497 plates with 10 nM of either pre-miR-34a-5p or si-miR-34a-5p^{Seed} with their respective controls. The
498 transfection mix was replaced 24 hours after transfection. Cells were lysed 48 hours after transfection using
499 Qiazol. For the RNA-Seq data in **Supplementary Figure 9**, HeyA8 cells were seeded at 50,000 cells per
500 well in a 6-well plate and treated with three genotoxic drugs in duplicate: carboplatin (25 µg/ml),
501 doxorubicin (50 ng/ml), and etoposide (500 nM). Medium treated cells were used as control for carboplatin
502 and doxorubicin treated cells. Solvent control treated cells (0.025% DMSO in medium) were used as control
503 for etoposide. Cells were lysed after 80 hours drug incubation using Qiazol. Total RNA was isolated using
504 the miRNeasy Mini Kit (Qiagen, Cat.No# 74004) following the manufacturer's instructions. An on-column
505 digestion step using the RNAse-free DNAse Set (Qiagen, Cat.No# 79254) was included for all RNA-Seq

506 samples. RNA libraries were generated and sequenced (Genomics Core facility at the University of
507 Chicago). The quality and quantity of the RNA samples were checked using an Agilent bio-analyzer. Paired
508 end RNA-SEQ libraries were generated using Illumina TruSEQ TotalRNA kits using the Illumina provided
509 protocol (including a RiboZero rRNA removal step). Small RNA-SEQ libraries were generated using
510 Illumina small RNA SEQ kits using the Illumina provided protocol. Two types of small RNA-SEQ sub-
511 libraries were generated: one containing library fragments 140–150 bp in size and one containing library
512 fragments 150–200 bp in size (both including the sequencing adaptor of about 130 bp). All three types of
513 libraries (one RNA-SEQ and two small RNA-SEQ) were sequenced on an Illumina HiSEQ4000 using
514 Illumina provided reagents and protocols. Adaptor sequences were removed from sequenced reads using
515 TrimGalore (https://www.bioinformatics.babraham.ac.uk/projects/trim_galore), The trimmed reads were
516 aligned to the hg38 version of the human genome, using either Tophat v2.1.0 (RNA-Seq data in
517 **Supplementary Figure 9**) or STAR v2.5.2 (RNA-Seq data in **Fig. 5a**). In either case, aligned reads were
518 associated with genes using HTSeq v0.6.1, and the UCSC hg38 transcriptome annotation from
519 iGenomes. Differentially expressed genes were identified using the edgeR R package.
520

521 **Arrayed real-time PCR**

522 The top 30 most downregulated survival genes shared among HeyA8 cells treated with carboplatin,
523 doxorubicin, and etoposide based on the RNA-Seq analysis were selected for a kinetics analysis using real-
524 time PCR. To prepare the RNAs for the kinetics analysis, 75,000/plate HeyA8 cells were plated in 15 cm
525 plates. Twenty-four hours after plating, one plate of HeyA8 cells were lysed in QIAzol as the control sample.
526 The rest of the plates were treated with 50 ng/ml doxorubicin for 7 hrs, 14.5 hrs, and 21 hrs respectively
527 before being lysed in QIAzol. To perform the arrayed real-time PCR, 200 ng total RNA per sample was used
528 as the input to make cDNA using the high-capacity cDNA reverse Transcription Kit (Applied Biosystems
529 #4368814). For TaqMan Low Density Array (TLDA) profiling, custom-designed 384-well TLDA cards
530 (Applied Biosystems, Cat. No#4346799) were selected and used according to the manufacturer's protocols.
531 For each sample, 20 µl cDNA was mixed with 80 µl water and 100 µl TaqMan Universal PCR Master Mix
532 (Applied Biosystems, Cat. No#4304437). A total volume of 100µl of each sample is loaded into the 8
533 loading ports on the TLDA card (2 ports for each sample, 4 samples total on one card). The qPCR assays
534 used to detect the 30 genes on the TLDA card are as follows: HIST1H2AI (Hs00361878_s1), CENPA
535 (Hs00156455_m1), HJURP (Hs00251144_m1), FAM72D (Hs00416746_m1), CCNA2 (Hs00996788_m1),
536 KIF20A (Hs00993573_m1), PRC1 (Hs01597839_m1), KIF15 (Hs01085295_m1), BUB1B
537 (Hs01084828_m1), SCD (Hs01682761_m1), AURKA (Hs01582072_m1), NUF2 (Hs00230097_m1),
538 NCAPH (Hs01010752_m1), SPC24 (Hs00699347_m1), KIF11 (Hs00189698_m1), TTK (Hs01009870_m1),
539 PLK4 (Hs00179514_m1), AURKB (Hs00945858_g1), CEP55 (Hs01070181_m1), HMGCS1

540 (Hs00940429_m1), TOP2A (Hs01032137_m1), KIF23 (Hs00370852_m1), INCENP (Hs00934447_m1),
541 CDK1 (Hs00938777_m1), HIST2H2BE (Hs00269023_s1), KNL1 (Hs00538241_m1), NCAPD2
542 (Hs00274505_m1), RACGAP1 (Hs01100049_mH), SPAG5 (Hs00197708_m1), KNTC1 (Hs00938554_m1).
543 GAPDH (Hs99999905_m1) was used as the endogenous control. qPCR assay for individual gene was done
544 in technical triplicates on each TLDA cards. Statistically analysis was performed using Student's t test.
545

546 **Ago affinity peptide purification**

547 To express and purify the FLAG-GST-T6B WT and mutant, constructs were expressed in BL21-
548 Gold(DE3)pLysS competent cells (Agilent). Bacteria, induced with 1 mM Isopropyl β-D-1-
549 thiogalactopyranoside (IPTG), were grown in 1 L overnight at 18ºC to OD 0.6. The bacteria were
550 sedimented at 4000*g* for 15 min and resuspended in 25 ml GST-A buffer (1 mM 4-(2-aminoethyl)
551 benzenesulfonyl fluoride hydrochloride (AEBSF), 1 mM DTT in PBS) supplemented with 1 mg/mL
552 lysozyme (Sigma). Samples were sonicated three times for 3 min at 100% amplitude (Sonics, VCX130) and
553 cleared by centrifugation at 20,000*g* for 20 min. The lysate was loaded onto a column containing 2 ml of
554 bead volume glutathione Sepharose beads (Sigma) and washed two times with GST-A buffer. The GST-
555 tagged protein was eluted in 10 ml of GST-B buffer (20 mM Tris, pH 8.0, and 10 mM glutathione in PBS).
556 The peptide was concentrated using Amicon Ultra-15 Centrifugal Filter Unit (Millipore) and desalted using
557 Zeba Spin Desalting Columns (ThermoFisher).
558

559 **Ago pull down and small RNA-seq**

560 HeyA8 (5-7 x 10^6), HCT116 wild-type (1.2-1.6 x 10^8) or *Drosha* k.o. (4.8-6.3 x 10^7) cells treated with
561 doxorubicin were lysed in NP40 lysis buffer (20 mM Tris, pH 7.5, 150 mM NaCl, 2 mM EDTA, 1% (v/v)
562 NP40, supplemented with phosphatase inhibitors) on ice for 15 minutes. The lysate was sonicated 3 times for
563 30 s at 60% amplitude (Sonics, VCX130) and cleared by centrifugation at 12,000*g* for 20 minutes. AGO1-4
564 were pulled down by using 500 µg of Flag-GST-T6B peptide [42] and with 60 µl anti-Flag M2 magnetic beads
565 (Sigma-Aldrich) for 2 hrs at 4°C. The pull-down was washed 3 times in NP40 lysis buffer. During the last
566 wash, 10% of beads were removed and incubated at 95°C for 5 minutes in 2x SDS-PAGE sample buffer.
567 Samples were run on a 4-12% SDS-PAGE and transferred to nitrocellulose membrane. The pull-down
568 efficiency was determined by immunoblotting against AGO2 (Abcam 32381). To the remaining beads 500
569 µl TRIzol reagent were added and the RNA extracted according to the manufacturer's instructions. The RNA
570 pellet was diluted in 20 µl of water. The sample was split and half of the sample was dephosphorylated with
571 0.5 U/µl of CIP alkaline phosphatase at 37°C for 15 min and subsequently radiolabeled with 0.5 µCi γ-^{32}P-
572 ATP and 1 U/µl of T4 PNK kinase for 20 min at 37°C. The AGO1-4 interacting RNAs were visualized on a
573 15% urea-PAGE. To prepare a small RNA library, RNA was ligated with 3' adenylated adapters and

separated on a 15% denaturing urea-PAGE. The RNA corresponding to insert size of 19-35 nt was eluted from the gel, ethanol precipitated followed by 5' adapter ligation. The samples were separated on a 12% Urea-PAGE and extracted from the gel. Reverse transcription was performed using Superscript III reverse transcriptase and the cDNA amplified by PCR. The cDNA was sequenced on Illumina HiSeq 3000.

Adapter sequences:

Adapter 1 – NNTGACTGTGGAATTCTCGGGTGCCAAGG;

Adapter 2 – NNACACTCTGGAATTCTCGGGTGCCAAGG,

Adapter 3 – NNACAGAGTGGAATTCTCGGGTGCCAAGG,

Adapter 4 – NNGCGATATGGAATTCTCGGGTGCCAAGG,

Adapter 47 – NNTCTGTGTGGAATTCTCGGGTGCCAAGG,

Adapter 48 – NNCAGCATTGGAATTCTCGGGTGCCAAGG,

Adapter 49 – NNATAGTATGGAATTCTCGGGTGCCAAGG,

Adapter 50 – NNTCATAGTGGAATTCTCGGGTGCCAAGG.

RT primer sequence: GCCTTGGCACCCGAGAATTCCA;

PCR primer sequences:

CAAGCAGAAGACGGCATACGAGATCGTGATGTGACTGGAGTTCCTTGGCACCCGAGAATTCCA.

Data analyses

GSEA was performed using the GSEA software version 3.0 from the Broad Institute downloaded from https://software.broadinstitute.org/gsea/. A ranked list was generated by sorting genes according the Log_{10}(fold downregulation). The Pre-ranked function was used to perform GSEA using the ranked list. 1000 permutations were used. Default settings were used. The ~1800 survival genes and ~420 non-survival genes defined previously [20] were used as custom gene sets. Default settings were used.

The list of survival genes and expression matched non-survival genes were generated by taking the survival and expression matched non-survival genes used previously (*20*) and retaining only the 938 genes in each group of expression matched survival and non-survival genes with an average expression across all RNA seq datasets above 1000 RPMs (see **Supplementary Data File 6**).

Sylamer analysis [29] was used to find enrichment of small word motifs in the 3'UTRs of genes enriched in those that are most downregulated. 3'UTRs were used from Ensembl, version 76. As required by Sylamer, they were cleaned of low-complexity sequences and repetitive fragments using respectively Dust [55] with default parameters and the RSAT interface [56] to the Vmatch program, also run with default parameters. Sylamer (version 12–342) was run with the Markov correction parameter set to 4. Bonferroni adjusted p-values were calculated by multiplying the unadjusted p-values by the number of permutations for each length of word searched for.

608 The GO enrichment analyses shown in **Fig. 5b** and **Supplementary Figure 6b** were performed using
609 the GOrilla GO analysis tool at http://cbl-gorilla.cs.technion.ac.il using default setting using different p-value
610 cut-offs for each analysis. GO analysis in **Supplementary Data File 5** was done using DAVID 6.8
611 (https://david.ncifcrf.gov) using default settings. GO analyses across multiple data sets were performed using
612 the software available on www.Metascape.org and default running parameters.

613 Density plots showing the contribution of the four nucleotides G, C, A and U at each of the 6mer seed
614 positions were generated using the Weblogo tool at http://weblogo.berkeley.edu/logo.cgi using the frequency
615 plot setting.

616 Venn diagrams were generated using http://bioinformatics.psb.ugent.be/webtools/Venn/ using default
617 settings.

618 The scatter plot in **Fig. 5a** was generated using R package ggplot2. 10875 genes with RPM > 1 (average
619 RPM of the 8 RNAseq samples) and adjusted p-value < 0.05 were included. 3696 genes were significantly
620 upregulated in both mir-34a-5p and si34a-5p^{Seed} treated samples. 4207 genes were significantly
621 downregulated in both mir-34a-5p and si34a-5p^{Seed} treated samples. 713 genes were only downregulated and
622 792 genes were only upregulated in si34a-5p^{Seed} treated samples. 730 genes were only downregulated and
623 737 genes were only upregulated in mir-34a-5p treated samples. 193 genes out of the total 10875 genes were
624 omitted in the graph as the range for X and Y axes were set as -3 to 3.

625

626 **Identification of the most and least toxic 6mer seeds**

627 To identify the 20 and 100 most and least toxic seeds to both human cell lines all 4096 seeds were ranked for
628 each cell line from highest to lowest toxicity. The 20 seeds with the highest toxicity to both HeyA8 and
629 H460 cells were found in the top 46 most toxic seeds to in both cells and the 20 seeds shared to be least toxic
630 were found in the bottom 149 seeds in each ranked group. The 100 most and least toxic seeds for both cell
631 lines were identified in the same way and all groups of seeds are shown in **Supplementary Data File 2**.

632

633 **Metaplots of 6-mer seed match locations**

634 3'UTR sequences were downloaded from Ensembl Biomart. In order to reduce redundancy in the sequences,
635 a single longest 3'UTR (and associated transcript) was chosen to represent each gene. A custom perl script
636 (makeSeedBed.pl) was written to identify exact matches to all seeds (reverse complement) in all sequences,
637 and to output the coordinates of those matches in bed file format. A custom R script (plotBedMetaPlot.R)
638 was written that uses the GenomicRanges [57] and Sushi [58] R packages to calculate the coverage of seeds
639 across all sequences in a given set, and to create a plot of that coverage. The custom scripts and the input
640 data are available in the cloud-based computational reproducibility platform Code Ocean at
641 https://codeocean.com/capsule/31ec8deb-8282-4a90-98e6-b80a0ba881cb/code.

642

643 **eCDF plots**

644 A custom perl script (annotateWithSeeds.pl) was written to identify exact seed matches (reverse
645 complement) to all seeds in all sequences, and to output the total counts of the different types of seeds
646 (generally toxic vs. nontoxic) in the sequences. To compare the presence of toxic and nontoxic seed matches
647 in expression matched survival and non survival genes, a custom R script (makeECDFplot.180615.R) was
648 written that takes as input two different sets of genes (SGs and nonSGs) and the list of the counts of toxic
649 and nontoxic seeds (reverse complement) in all genes, and plots the cumulative distribution function for the
650 count statistics in each gene set. In **Fig. 3b** the ratio of the seed match counts to the 20 most and least toxic
651 seeds in the 5'UTR, CDS, first 1000bp of 3'UTR, and full 3'UTR (not shown) were compared between pairs
652 of 938 expression matched survival and non-survival genes. In **Supplementary Figure 5a**, this analysis was
653 repeated with the 100 most and least toxic seeds to both human cell lines. The custom scripts and the input
654 data are available in the cloud-based computational reproducibility platform Code Ocean at
655 https://codeocean.com/capsule/b755ec2b-00d8-4281-9fa1-2a484fd7521b/code. To determine the dependence
656 of mRNAs regulation on miR-34a-5p seed presence in their 3'UTR, a custom R script
657 (makeECDFplot.cetoData.R) was written that takes as input a list of gene sets and a table of logFC
658 expression for those genes upon miR-34a-5p or si34a-5p^{Seed} over-expression. This Rscript then plots the
659 cumulative distribution function for the logFC expression data in each gene set. The custom scripts and the
660 input data are available in the Code Ocean at https://codeocean.com/capsule/31ec8deb-8282-4a90-98e6-
661 b80a0ba881cb/code.

662

663 **Relation between miRNA seed conservation, age and toxicity**

664 Information on miRNA seed family conservation and seed sequence were downloaded at
665 http://www.targetscan.org/vert_71/ from TargetScan Human 7.1. The toxicity of each mature human miRNA
666 arm sequence in the TargetScan dataset was assigned according to the average toxicity induced by the
667 siRNA in HeyA8 and H460 siRNA screens harboring the identical 6mer seed sequence. A list of miRNA
668 ages corresponding to ~1025 miRNA loci was acquired from [31] and was calculated using a modified version
669 of ProteinHistorian [31]. This list was used to assign ages to roughly ~1400 mature miRNA arms found in the
670 TargetScan dataset.

671 TargetScan 7.1 partitions the seed family conservation into four groups: highly conserved (group #2),
672 conserved (group #1), low conservation but still annotated as a miRNA (group #0), and low conservation
673 with the possibility of misannotation (group #-1). Probability density and eCDF plots for the assigned 6mer
674 seed-dependent toxicities were generated for each seed family conservation group as defined by Targetscan
675 (groups -1, 0, 1, and 2) using ggplot2 in R. Probability density and eCDF plots were also generated to show

676 how young (<10 million years) and old (>800 million years) miRNAs compare in terms of the seed-
677 dependent toxicity. All differences between groups in terms of seed-dependent toxicity (always the average
678 of the toxicity determined in HeyA8 and H460 cells) were analyzed using a two-sample two-tailed
679 Kolmogorov-Smirnov test in R.
680

681 **Assessment of dominant arm seed toxicity**

682 The expression (RPM) of miRNA 5p and 3p arms across 135 tissue samples were collected from MIRMINE
683 [59]. A miRNA was considered expressed if the sum of the normalized reads for both arms was above 5 for
684 each sample. A value of 0 was replaced with 0.01 to avoid a division by 0 error. A miRNA arm was
685 considered the dominant species if its expression was at least 25% greater than the other arm per sample. The
686 dominant arm for each miRNA across all samples was calculated by determining which arm was dominantly
687 expressed in more samples (>50% of samples where the miRNA was considered expressed). The miRNAs
688 that have only one annotated arm in miRBase were considered to have only one dominant arm. The seed
689 toxicity values for each arm were extracted from the 4096 siRNA screen data (% average viability for the
690 human HeyA8 and H460 cells) and used to calculate the ratio between the dominant arm's toxicity and the
691 lesser arm's toxicity; miRNAs that only had one expressed arm were not considered in the analyses shown in
692 **Fig. 6d** but are all included on the website: 6merdb.org.

693 To compare the 6mer seed toxicity between up regulated and down regulated Ago bound miRNA
694 populations in HCT116 cells after Doxo treatment we analyzed the reads obtained from RNA Seq analysis of
695 Ago bound RNAs. After removing the reads that were either shorter than 19 nt or longer than 26 nt in length,
696 the reads were blasted against a miRNA database consisting of all human miRNA mature sequence
697 information obtained from miRBase. A threshold of 100% identity for an at least 16 nt-long stretch without
698 any gaps was set for the BLAST analysis. After discarding sequences with no significant BLAST result, the
699 remaining sequences were trimmed from the 3'end so that all reads were now 19nt in length. This was done
700 to determine for each miRNA the relevant 5' end to obtain the 6mer seed sequence (position 2-7). All the
701 reads that shared the same 5' sequence and miRNA names were collapsed while adding up the number of
702 reads of each sequence in each condition. To compare the 6mer seed toxicity between up and down regulated
703 miRNAs, we calculated the average 6mer seed toxicity for miRNA sequences that were either 1.5 fold up or
704 1.5 fold down regulated in Doxo treated wt samples compared to medium treated control samples (after
705 removing sequences that had less than 100 collapsed reads in Doxo treated wt samples). In each group
706 miRNAs were ranked according to highest base mean expression and groups were compared (**Fig. 7d**).
707 Statistically significance was determined using the Wilcoxon rank test. The comparison was repeated for
708 *Drosha* k.o. cells where the 5' shifted form of miR-320a-3p was the only miRNA found to be upregulated
709 (1.5 fold).

710

711 **Analysis of miRtron and non-miRtron groups**

712 MiRtrons and non-miRtrons were recently reported [60] and consisted of miRNAs that are listed in miRBase
713 v21 as expressing both arms. Comparing 6mer toxicity of miRtrons and non-miRtrons from this list was
714 done as described above for young/old non-conserved/conserved miRNAs. Both arms were considered.
715 Probability density (**Fig. 6c**) and eCDF plots (**Supplementary Figure 7c**) were generated to show how
716 miRtrons and non-miRtrons compare in terms of the seed-dependent toxicity. To calculate the 6mer toxicity
717 across the entire miRtron sequences, we extracted all possible 6-nt stretches from the first 17nts of the 428
718 mature miRtron sequences beginning at the 5'end using a 6nt sliding window (12 different start positions in
719 total). The first 17nts were chosen because all miRtrons sequences are 17-25nt in length. Average 6mer
720 toxicity of the 428 miRtrons was calculated for each start position and plotted in **Supplementary Figure 7e**.
721 To visualize the nucleotide content across of all miRtrons, the first 8 nucleotides from the 5'end or the last 8
722 nucleotides from the 3'end were extracted from the 428 mature miRtron sequences and analyzed using the
723 Weblogo tool.
724

725 **Seed viability of shRNAs derived from the CD95L sequence**

726 An RNAi lethality screen composed of every shRNA sequence that can be derived from the CD95L CDS
727 was conducted previously (*20*). In this screen, toxicity of each shRNA was assessed in two ways: 1) fold
728 underrepresentation of the shRNA after infection with the shRNA-expressing lentivirus compared to its
729 representation in the plasmid pool and 2) fold representation of the shRNA after infection and treatment with
730 doxycycline compared to cells that were infected but did not receive doxycycline. The first analysis allowed
731 us to quantify toxicity associated with leaky shRNA expression. The second analysis quantified toxicity
732 associated with strong shRNA expression following treatment with doxycycline.

733 For each shRNA, the average fold downregulation was calculated from both of these toxicity assessments.
734 Then, the seed sequence of each shRNA was extracted and assigned an average viability score, which was a
735 composite of the % viabilities determined in the 4096 siRNA arrayed screen for both HeyA8 and H460 cells.

736 Pearson's correlation was determined for each CD95L-derived shRNA between its associated fold
737 downregulation in the screen (*20*) and the average seed sequence viability determined in the 4096 siRNA
738 screen.

739 In addition, the CD95L shRNAs were split into two groups: 1) 137 shRNAs with an average fold
740 downregulation (as determined in the shRNA lethality screen) above 5 and 2) a control group with a
741 matching number of shRNAs whose fold deregulation had an absolute value closest to 0. The average seed
742 viability (as determined from the siRNA screen) was extracted for the shRNAs in these two groups and
743 compared using the two-sample, two-tailed Rank Sum test.
744

745 **Statistical analyses**

Continuous data were summarized as means and standard deviations (except for all IncuCyte experiments where standard errors are shown) and dichotomous data as proportions. Continuous data were compared using t-tests for two independent groups and one-way ANOVA for 3 or more groups. For evaluation of continuous outcomes over time, two-way ANOVA was performed using the Stata 14 software with one factor for the treatment conditions of primary interest and a second factor for time treated as a categorical variable to allow for non-linearity. Comparisons of single proportions to hypothesized null values were evaluated using binomial tests. Statistical tests of two independent proportions were used to compare dichotomous observations across groups. Pearson correlation coefficients (r) and p - values as well as Wilcoxon rank test were calculated using StatPlus (v. 6.3.0.5). Kolmogorov–Smirnov two-sample two-sided test was used to compare different probability distributions shown in all density plots and eCDF plots. Wilcoxon rank sum test was used to test for statistical significance in the analysis of the toxicity all miRNA arms in **Fig. 6d**. The Fisher Exact Test was used to calculate p-values in **Fig. 6b** to determine whether the percent frequency of G versus non-G (A, C, and U) nucleotides at each position along the 6mer seed was different between young (<10M years) and ancient (>800M years) miRNAs. The effects of treatment vs. control over time were compared for *Drosha* k.o. and wild-type cells by fitting regression models that included linear and quadratic terms for value over time, main effects for treatment and cell type, and two- and three-way interactions for treatment, cell-type and time. The three-way interaction on the polynomial terms with treatment and cell type was evaluated for statistical significance since this represents the difference in treatment effects over the course of the experiment for the varying cell types.

Data availability

RNA sequencing data generated for this study is available in the GEO repository: GSE111379 (https://www.ncbi.nlm.nih.gov/geo/query/acc.cgi?acc=GSE111379, reviewer access token: srileyyktjctduz) and GSE111363 (https://www.ncbi.nlm.nih.gov/geo/query/acc.cgi?acc=GSE111363, reviewer access token: udedukauvjexbmp). All 6mer seed toxicity data of the 4096 siRNA screen in HeyA8, H460, M565, and 3LL cells are available in searchable form at https://6merdb.org. All source data are available upon request.

ACKNOWLEDGEMENTS

We are indebted to Dr. Leon Platanias for his generous support of the seed screen and to Denise Scholtens for help with biostatistics. M.H. was supported by the Intramural Research Program of NIAMS and A.A.S. by the Swedish Research Council postdoctoral fellowship. This work was funded by training grant T32CA009560 (to W.P.), R35CA197450 (to M.E.P.), R50CA221848 (to E.T.B.), and RO1 211916 (to EL).

AUTHOR CONTRIBUTIONS

M.E.P., Q.Q.G., W.E.P. and A.E.M. conceived the study. Q.Q.G., W.E.P. performed the majority of the experiments and data analysis. S.C. performed the 6mer seed screens. A.A.S. performed the Ago pull-down experiments. E.T.B. performed data analyses. J.M.P designed and implemented the website. M.H. provided critical conceptual input. M.E.P. designed the study, guided the interpretation of the results and drafted the manuscript. All authors discussed the results, edited and approved the draft and final versions of the manuscript.

DECLARATION OF INTEREST

The authors declare no competing interests.

792 **Figure legends**

793

794 **Fig. 1** A comprehensive screen identifies the most toxic 6mer seeds. **a** Schematic of the siRNA backbone
795 used in the 4096 seed duplexes toxicity screen. Red X: 2'-O-methylation modification; blue letters: constant
796 nucleotides; red letters: variable 6mer seed sequence. **b** *Top:* Results of the 4096 6mer seed duplex screen in
797 two human (top) and two mouse (bottom) cell lines. Cells were reverse transfected in triplicates in 384 well
798 plates with 10 nM of individual siRNAs. The cell viability of each 6mer seed duplex was determined by
799 quantifying cellular ATP content 96 hours after transfection. All 4096 6mer seeds are ranked by the average
800 effect on cell viability of the four cell lines from the most toxic (left) to the least toxic (right). Rankings of
801 the 6mer seeds of four previously characterized CD95L derived siRNAs (siL1, siL2, siL3, and siL4) are
802 highlighted in green. We consider an siRNA highly toxic if it reduces cell viability 90% or more and
803 moderately toxic if it reduces cell viability 50% or more (black stippled line). **c** Regression analysis showing
804 correlation between the 6mer seed toxicity observed in the human lung cancer cell line H460 (y axis) and the
805 matching 6mer toxicity observed in the human ovarian cancer cell line HeyA8 (x axis) (left) and average
806 toxicity in the two human cell lines (y axis) and two mouse cell lines (x axis) (right). p-values were
807 calculated using Pearson correlation analysis. **d** *Left:* Correlation between the $\log_{10}$ (fold down
808 underrepresentation) of all possible shRNAs that can be derived from the mRNA sequence of CD95L
809 following their expression from a DOX-inducible lentiviral vector [20] and the toxicity of their seed sequences
810 as determined in a 4096 arrayed siRNA screen (average of both human cell lines). *Right*: Difference in
811 average seed toxicity between the 137 CD95L-derived shRNAs downregulated at least 5 fold (= toxic) in this
812 screen compared to a size matched group of 137 shRNAs that were the least altered in abundance in that
813 screen. Pearson correlation coefficient is given as well as p-value (left) and p-value in analysis on the right
814 was calculated using unpaired two-sided ttest. The center crossbar of the box plot represents the mean, and
815 the upper/lower boundaries demark +/- 1 standard deviation.

816

817 **Fig. 2** The most toxic seeds are G rich. **a** Cell viability of the 19 seed duplexes with the highest content
818 (>80%) in the 6mer seed region for each nucleotide in two human and two mouse cell lines. Samples were
819 analyzed in triplicate and mean ± SD for each sample is shown. p-values between groups of duplexes were
820 calculated using Student's t-test. **b** Nucleotide composition at each of the 6 seed positions in the top 200 most
821 toxic (left) or the top 200 least toxic (right) seed duplexes in the four cell lines. siRNAs are considered to be
822 toxic when viability is inhibited >50% (grey stippled line).

823

824 **Fig. 3** Toxic G-rich seed-containing duplexes target housekeeping genes enriched in Cs. **a** Nucleotide
825 composition of 20 seeds that are most and least toxic in both human cell lines (see **Fig. 1b**). **b** eCDF

comparing the ratio of occurrences of the 20 most and least toxic 6mer seed matches in the mRNA elements of two sets of expression matched survival genes and nonsurvival genes. Significance was calculated using a two-sample two-sided Kolmogorov–Smirnov (K-S) test. **c** Probability density plots comparing the nucleotide content between the groups of expression matched SGs and nonSGs. p-values were calculated using a two-sample two-sided K-S test comparing the density distribution of SGs and nonSGs. Relevant peak maxima are given. **d** Single nucleotide frequency distribution in human mRNAs around the boundaries of the 5'UTR and the beginning of the CDS and the end of the CDS and the beginning of the 3'UTR (shown are 500 bases in each direction). Data are shown for either all human coding genes (top), or a set of 938 SGs or an expression matched set of 938 nonSGs (bottom four panels). Blue horizontal bars, area of reduced A/U content in SGs. p-values were calculated using a two-sample two-sided K-S test. **e** Distribution of the seed matches to the 20 most and least toxic 6mer seeds to human cells in human mRNAs around the boundaries of the 5'UTR and the beginning of the CDS and the end of the CDS and the beginning of the 3'UTR (shown are 500 bases in each direction). Data are shown for either all genes (top) or the expression matched SGs and nonSGs (center and bottom). Green horizontal bar, area of enriched toxic seed matches in SGs compared to nonSGs. Blue horizontal bar, area of fewer toxic seed matches in SGs.

Fig. 4 Tumor suppressive miRNAs inhibit cancer cell growth via toxic 6mer seeds. **a** All 4096 6mer seeds ranked from the lowest average viability (highest toxicity) to the highest viability (lowest toxicity) in HeyA8 and H460 cells. Locations of 6mer seeds present in major tumor suppressive (red) or tumor promoting (blue) miRNAs are highlighted as individual bars. miRNAs are considered to be toxic when viability is inhibited >50% (blue stippled line). **b** Percent cell confluence over time of HeyA8 cells transfected with 5 nM of either the indicated tumor suppressive miRNA precursors or a miRNA precursor nontargeting control. Data are representative of two independent experiments. Each data point represents mean ± SE of four replicates. *Two-way ANOVA p-value between cells treated with pre-miR-(NC) and pre-let-7a-5p is 0.0000. **c** *Left*: Percent cell confluence over time of HeyA8 parental cells transfected with either pre-miR-34a-5p or si34a-5p^{Seed} and compared to their respective controls (pre-miR (NC) for pre-miR-34a-5p and siNT2 for si34a-5p^{Seed}) at 10 nM. Data are representative of two independent experiments. Each data point represents mean ± SE of four replicates. *Right*: % cell death of the same cells harvested 4 days after transfection. Data are representative of two experiments. Each data point represents mean ± SD of three replicates. **d** Morphology of HeyA8 cells transfected with 10 nM of either pre-miR-34a-5p or si34a-5p^{Seed} compared to their respective controls three days after transfection.

Fig. 5 miR-34a-5p kills cancer cells through its toxic 6mer seed. **a** *Top*: Alignment of the sequences of miR-34a-5p and miR-34a-5p^{Seed} with the 6mer highlighted. *Bottom:* Comparison of deregulated mRNAs

860 (adjusted $p<0.05$, RPM > 1) in HeyA8 cells 48 hrs after transfection with either miR-34a-5p or si34a-
861 $5p^{Seed}$. Pearson correlation p-value is given. **b** Overlap of RNAs detected by RNA-Seq downregulated in
862 HeyA8 cells (>1.5 fold) 48 hrs after transfection with either si34a-$5p^{Seed}$ or miR-34a-5p when compared to
863 either siNT2 or a nontargeting pre-miR, respectively. *Right*: Results of a GOrilla gene ontology analyses of
864 the genes downregulated in both cells transfected with miR-34a-5p or si34a-$5p^{Seed}$ (top, significance of
865 enrichment $<10^{-11}$), or only in cells transfected with miR-34a-5p (bottom, significance of enrichment $<10^{-4}$).
866 **c** Sylamer plots for the list of 3'UTRs of mRNAs in cells treated with either miR-34a-5p (top) or si34-$5p^{Seed}$
867 (bottom) sorted from down-regulated to up-regulated. The most highly enriched sequence is shown which, in
868 each case, is the 6mer seed match of the introduced 6mer seed. Bonferroni-adjusted p-values are shown. **d**
869 Gene set enrichment analysis for a group of 1846 survival genes (top 4 panels) and 416 non-survival genes
870 (bottom 2 panels) [20] after transfecting HeyA8 cells with either miR-34a-5p or si34a-$5p^{Seed}$. siNT1 and a
871 nontargeting premiR served as controls, respectively. p-values indicate the significance of enrichment.
872
873 **Fig. 6** Toxic 6mer seeds and the evolution of cancer regulating miRNAs. **a** Probability density plot of cell
874 viability of the 6mer seeds of either highly conserved (from humans to zebrafish) or poorly conserved
875 miRNA seed families (left panel, total number of mature miRNAs = 2164) or of very old (>800 Million
876 years) miRNAs or very young (<10 Million years) miRNAs (right panel, total number of miRNAs = 299).
877 For the analysis on the right, miRNA arms with identical sequences (gene duplications) were collapsed and
878 counted as one arm. Two-sample two-sided K-S test was used to calculate p-values. **b** Change in nucleotide
879 composition in the 6mer seeds of miRNAs of different ages. Significance of change in nucleotide
880 composition at each of the 6 seed positions between the youngest and oldest miRNAs was calculated using a
881 Fisher's exact test. Note: the oldest miRNAs also contain tumor suppressive miRNAs with high G content in
882 positions 1 and 2 which may be the reason the analysis in these two positions did not reach statistical
883 significance. **c** Probability density plot of cell viability of the 6mer seeds of mature miRtrons or non-
884 miRtrons. miRNAs with identical sequences (gene duplications) were collapsed and counted as one seed.
885 Two-sample two-sided K-S test was used to calculate p-value. **d** 780 miRNAs (**Supplementary Data File 4**)
886 ranked according to the ratio of viability of the seed (as determined in the seed screen) of the guide strand
887 and the lesser-expressed arm. Established oncogenic miRNAs are shown in blue, tumor-suppressive
888 miRNAs are shown in red. The guide strand is given for each miRNA (in parenthesis). p-value of the
889 distribution of oncogenic versus tumor suppressive miRNAs was calculated using Wilcoxon rank test. **e**
890 Cumulative read numbers from the 5p or the 3p arm (according to miRBase.org) of three oncogenic and
891 three tumor-suppressive miRNAs with the highest (top three) or lowest (bottom three) ratio of the viability of
892 the guide strand versus the lesser arm. The viability numbers of the matching 6mer seeds according to the

siRNA 6mer seed screen are given. The sequences of the mature 5p or 3p arms are boxed in blue and black, respectively. Toxic seeds are shown in red, non-toxic ones in blue.

Fig. 7 Genotoxic drugs cause upregulation of tumor suppressive miRNAs with toxic 6mer seeds. **a** *Top*: Autoradiograph of radiolabeled RNAs pulled down with the Ago proteins from HeyA8 cells treated with doxorubicin (Doxo) for different times. *Bottom*: Western blot for the pulled down AGO2 of the same samples shown above. The images are representative of two biological duplicates. **b** Fold change of the total reads of Ago bound small RNAs after 20, 40, or 80 hours of Doxo treatment compared to the control sample from Ago-IP sequencing data (Ago bound). Fold change of the total reads of cytosolic small RNAs in HeyA8 cells treated with Doxo for 80 hours compared to the control sample from small RNA-Seq data is given (Total). Data are the combination of biological duplicates. **c** Pie charts showing the composition of miRNAs bound to Ago proteins after 50 hrs Doxo treatment in HCT116 wild-type (left) or *Drosha* k.o. cells (right). **d** *Left*, 6mer seed viability (average between HeyA8 and H460 cells, two replicates) of the Ago-bound miRNAs most up and downregulated in wt or *Drosha* k.o. cells after Doxo treatment. K-S test was used to calculate p-value. *Right*, Comparison of the predicted (and most abundant) sequence of miR-320a-3p and Ago-bound sequence of miR-320a-3p and their average viability found most upregulated in *Drosha* k.o. cells after Doxo treatment. Shown is variance of two biological replicates. **e** Percent cell confluence over time of HeyA8 cells transfected with 5 nM of controls, pre-miR-320a-3p or an siRNA duplex that corresponds to the shifted form of miR-320a-3p (si-miR-320a-3p^{Ago}) that was found to be upregulated and bound to Ago proteins upon Doxo treatment. Data are representative of two independent experiments. Each data point represents mean ± SE of four replicates. **f** Viability changes (ATP content) in four cell lines 96 hrs after transfection with Lipid only, 10 nM of siNT1, siL3, a nontargeting pre-miR, or miR-320a-3p^{Ago} - the only shared upregulated miRNA in HeyA8 cells, HCT116 wild-type, and HCT116 *Drosha* k.o. cells - after Doxo treatment. p-values were determined using Student's t-test. *** $p<0.0001$. Samples were performed in triplicate (siNT1, siL3), 6 repeats (miR-320a-3p^{Ago}) and 8 repeats (Lipid).

REFERENCES

1. Lee Y, *et al.* MicroRNA genes are transcribed by RNA polymerase II. *EMBO J* **23**, 4051-4060 (2004).

2. Han J, Lee Y, Yeom KH, Kim YK, Jin H, Kim VN. The Drosha-DGCR8 complex in primary microRNA processing. *Genes Dev* **18**, 3016-3027 (2004).

3. Yi R, Qin Y, Macara IG, Cullen BR. Exportin-5 mediates the nuclear export of pre-microRNAs and short hairpin RNAs. *Genes Dev* **17**, 3011-3016 (2003).

930 4. Bernstein E, Caudy AA, Hammond SM, Hannon GJ. Role for a bidentate ribonuclease in the
931 initiation step of RNA interference. *Nature* **409**, 363-366 (2001).
932
933 5. Hutvagner G, McLachlan J, Pasquinelli AE, Balint E, Tuschl T, Zamore PD. A cellular function for
934 the RNA-interference enzyme Dicer in the maturation of the let-7 small temporal RNA. *Science*
935 **293**, 834-838 (2001).
936
937 6. Wang Y, Sheng G, Juranek S, Tuschl T, Patel DJ. Structure of the guide-strand-containing
938 argonaute silencing complex. *Nature* **456**, 209-213 (2008).
939
940 7. Leuschner PJ, Ameres SL, Kueng S, Martinez J. Cleavage of the siRNA passenger strand during
941 RISC assembly in human cells. *EMBO Rep* **7**, 314-320 (2006).
942
943 8. Schirle NT, MacRae IJ. The crystal structure of human Argonaute2. *Science* **336**, 1037-1040
944 (2012).
945
946 9. Eulalio A, Huntzinger E, Izaurralde E. GW182 interaction with Argonaute is essential for
947 miRNA-mediated translational repression and mRNA decay. *Nat Struct Mol Biol* **15**, 346-353
948 (2008).
949
950 10. Lewis BP, Shih IH, Jones-Rhoades MW, Bartel DP, Burge CB. Prediction of mammalian
951 microRNA targets. *Cell* **115**, 787-798 (2003).
952
953 11. Lai EC. Micro RNAs are complementary to 3' UTR sequence motifs that mediate negative post-
954 transcriptional regulation. *Nat Genet* **30**, 363-364 (2002).
955
956 12. Selbach M, Schwanhausser B, Thierfelder N, Fang Z, Khanin R, Rajewsky N. Widespread changes
957 in protein synthesis induced by microRNAs. *Nature* **455**, 58-63 (2008).
958
959 13. Baek D, Villen J, Shin C, Camargo FD, Gygi SP, Bartel DP. The impact of microRNAs on protein
960 output. *Nature* **455**, 64-71 (2008).
961
962 14. Esquela-Kerscher A, Slack FJ. Oncomirs - microRNAs with a role in cancer. *Nat Rev Cancer* **6**,
963 259-269 (2006).
964
965 15. Balatti V, Pekarky Y, Rizzotto L, Croce CM. miR deregulation in CLL. *Adv Exp Med Biol* **792**, 309-
966 325 (2013).
967
968 16. Slabakova E, Culig Z, Remsik J, Soucek K. Alternative mechanisms of miR-34a regulation in
969 cancer. *Cell Death Dis* **8**, e3100 (2017).
970
971 17. Hua YJ, Larsen N, Kalyana-Sundaram S, Kjems J, Chinnaiyan AM, Peter ME. miRConnect 2.0:
972 Identification of antagonistic, oncogenic miRNA families in three human cancers. *BMC Genomics*
973 **14**, 179 (2013).
974
975 18. Concepcion CP, Bonetti C, Ventura A. The microRNA-17-92 family of microRNA clusters in
976 development and disease. *Cancer journal* **18**, 262-267 (2012).
977
978 19. He X, He L, Hannon GJ. The guardian's little helper: microRNAs in the p53 tumor suppressor
979 network. *Cancer Res* **67**, 11099-11101 (2007).

20. Putzbach W, *et al.* Many si/shRNAs can kill cancer cells by targeting multiple survival genes through an off-target mechanism. *eLife* **6**, e29702 (2017).

21. Murmann AE, *et al.* Induction of DISE in ovarian cancer cells in vivo. *Oncotarget* **8**, 84643-84658 (2017).

22. Murmann AE, *et al.* Small interfering RNAs based on huntingtin trinucleotide repeats are highly toxic to cancer cells. *EMBO Rep* **19**, e45336 (2018).

23. Putzbach W, *et al.* CD95/Fas ligand mRNA is toxic to cells. In revision. Preprint at BiorXiv. https://doi.org/10.1101/330324 (2018).

24. Hadji A, *et al.* Death induced by CD95 or CD95 ligand elimination. *Cell Reports* **10**, 208-222 (2014).

25. Bramsen JB, *et al.* A large-scale chemical modification screen identifies design rules to generate siRNAs with high activity, high stability and low toxicity. *Nucleic Acids Res* **37**, 2867-2881 (2009).

26. Peter ME. Let-7 and miR-200 microRNAs: guardians against pluripotency and cancer progression. *Cell Cycle* **8**, 843-852 (2009).

27. Agostini M, Knight RA. miR-34: from bench to bedside. *Oncotarget* **5**, 872-881 (2014).

28. Patel M, Peter ME. Identification of DISE-inducing shRNAs by monitoring cellular responses. *Cell Cycle* **17**, 506-514 (2018).

29. van Dongen S, Abreu-Goodger C, Enright AJ. Detecting microRNA binding and siRNA off-target effects from expression data. *Nat Methods* **5**, 1023-1025 (2008).

30. Grimson A, Farh KK, Johnston WK, Garrett-Engele P, Lim LP, Bartel DP. MicroRNA targeting specificity in mammals: determinants beyond seed pairing. *Mol Cell* **27**, 91-105 (2007).

31. Patel VD, Capra JA. Ancient human miRNAs are more likely to have broad functions and disease associations than young miRNAs. *BMC Genomics* **18**, 672 (2017).

32. Berezikov E, Chung WJ, Willis J, Cuppen E, Lai EC. Mammalian mirtron genes. *Mol Cell* **28**, 328-336 (2007).

33. Meijer HA, Smith EM, Bushell M. Regulation of miRNA strand selection: follow the leader? *Biochem Soc Trans* **42**, 1135-1140 (2014).

34. Concepcion CP, *et al.* Intact p53-dependent responses in miR-34-deficient mice. *PLoS Genet* **8**, e1002797 (2012).

35. Meredith AM, Dass CR. Increasing role of the cancer chemotherapeutic doxorubicin in cellular metabolism. *J Pharm Pharmacol* **68**, 729-741 (2016).

1029 36. Yeung TK, Germond C, Chen X, Wang Z. The mode of action of taxol: apoptosis at low
1030 concentration and necrosis at high concentration. *Biochem Biophys Res Commun* **263**, 398-404
1031 (1999).
1032
1033 37. Yoo SH*, et al.* Etoposide induces a mixed type of programmed cell death and overcomes the
1034 resistance conferred by Bcl-2 in Hep3B hepatoma cells. *Int J Oncol* **41**, 1443-1454 (2012).
1035
1036 38. Kwon HK*, et al.* Etoposide Induces Necrosis Through p53-Mediated Antiapoptosis in Human
1037 Kidney Proximal Tubule Cells. *Toxicol Sci* **148**, 204-219 (2015).
1038
1039 39. Wang D, Lippard SJ. Cellular processing of platinum anticancer drugs. *Nat Rev Drug Discov* **4**,
1040 307-320 (2005).
1041
1042 40. Chang BD*, et al.* A senescence-like phenotype distinguishes tumor cells that undergo terminal
1043 proliferation arrest after exposure to anticancer agents. *Cancer Res* **59**, 3761-3767 (1999).
1044
1045 41. Eom YW*, et al.* Two distinct modes of cell death induced by doxorubicin: apoptosis and cell
1046 death through mitotic catastrophe accompanied by senescence-like phenotype. *Oncogene* **24**,
1047 4765-4777 (2005).
1048
1049 42. Hauptmann J*, et al.* Biochemical isolation of Argonaute protein complexes by Ago-APP. *Proc*
1050 *Natl Acad Sci U S A* **112**, 11841-11845 (2015).
1051
1052 43. Kim YK, Kim B, Kim VN. Re-evaluation of the roles of DROSHA, Export in 5, and DICER in
1053 microRNA biogenesis. *Proc Natl Acad Sci U S A* **113**, E1881-1889 (2016).
1054
1055 44. Walz AL*, et al.* Recurrent DGCR8, DROSHA, and SIX homeodomain mutations in favorable
1056 histology Wilms tumors. *Cancer Cell* **27**, 286-297 (2015).
1057
1058 45. Kumar MS, Lu J, Mercer KL, Golub TR, Jacks T. Impaired microRNA processing enhances cellular
1059 transformation and tumorigenesis. *Nat Genet* **39**, 673-677 (2007).
1060
1061 46. Chandradoss SD, Schirle NT, Szczepaniak M, MacRae IJ, Joo C. A Dynamic Search Process
1062 Underlies MicroRNA Targeting. *Cell* **162**, 96-107 (2015).
1063
1064 47. Di Martino MT*, et al.* Synthetic miR-34a mimics as a novel therapeutic agent for multiple
1065 myeloma: in vitro and in vivo evidence. *Clin Cancer Res* **18**, 6260-6270 (2012).
1066
1067 48. Beg MS*, et al.* Phase I study of MRX34, a liposomal miR-34a mimic, administered twice weekly
1068 in patients with advanced solid tumors. *Invest New Drugs* **35**, 180-188 (2017).
1069
1070 49. Cao W*, et al.* miR-34a regulates cisplatin-induce gastric cancer cell death by modulating
1071 PI3K/AKT/survivin pathway. *Tumour Biol* **35**, 1287-1295 (2014).
1072
1073 50. Navarro F, Lieberman J. miR-34 and p53: New Insights into a Complex Functional Relationship.
1074 *PLoS One* **10**, e0132767 (2015).
1075
1076 51. Alfano L, Costa C, Caporaso A, Antonini D, Giordano A, Pentimalli F. HUR protects NONO from
1077 degradation by mir320, which is induced by p53 upon UV irradiation. *Oncotarget* **7**, 78127-
1078 78139 (2016).

52. Stark A, Brennecke J, Bushati N, Russell RB, Cohen SM. Animal MicroRNAs confer robustness to gene expression and have a significant impact on 3'UTR evolution. *Cell* **123**, 1133-1146 (2005).

53. Zare H, Khodursky A, Sartorelli V. An evolutionarily biased distribution of miRNA sites toward regulatory genes with high promoter-driven intrinsic transcriptional noise. *BMC Evol Biol* **14**, 74 (2014).

54. Ceppi P*, et al.* CD95 and CD95L promote and protect cancer stem cells. *Nature Commun* **5**, 5238 (2014).

55. Morgulis A, Gertz EM, Schaffer AA, Agarwala R. A fast and symmetric DUST implementation to mask low-complexity DNA sequences. *J Comput Biol* **13**, 1028-1040 (2006).

56. Medina-Rivera A*, et al.* RSAT 2015: Regulatory Sequence Analysis Tools. *Nucleic Acids Res* **43**, W50-56 (2015).

57. Lawrence M*, et al.* Software for computing and annotating genomic ranges. *PLoS Comput Biol* **9**, e1003118 (2013).

58. Phanstiel DH, Boyle AP, Araya CL, Snyder MP. Sushi.R: flexible, quantitative and integrative genomic visualizations for publication-quality multi-panel figures. *Bioinformatics* **30**, 2808-2810 (2014).

59. Panwar B, Omenn GS, Guan Y. miRmine: a database of human miRNA expression profiles. *Bioinformatics* **33**, 1554-1560 (2017).

60. Rorbach G, Unold O, Konopka BM. Distinguishing mirtrons from canonical miRNAs with data exploration and machine learning methods. *Sci Rep* **8**, 7560 (2018).

Figure 1

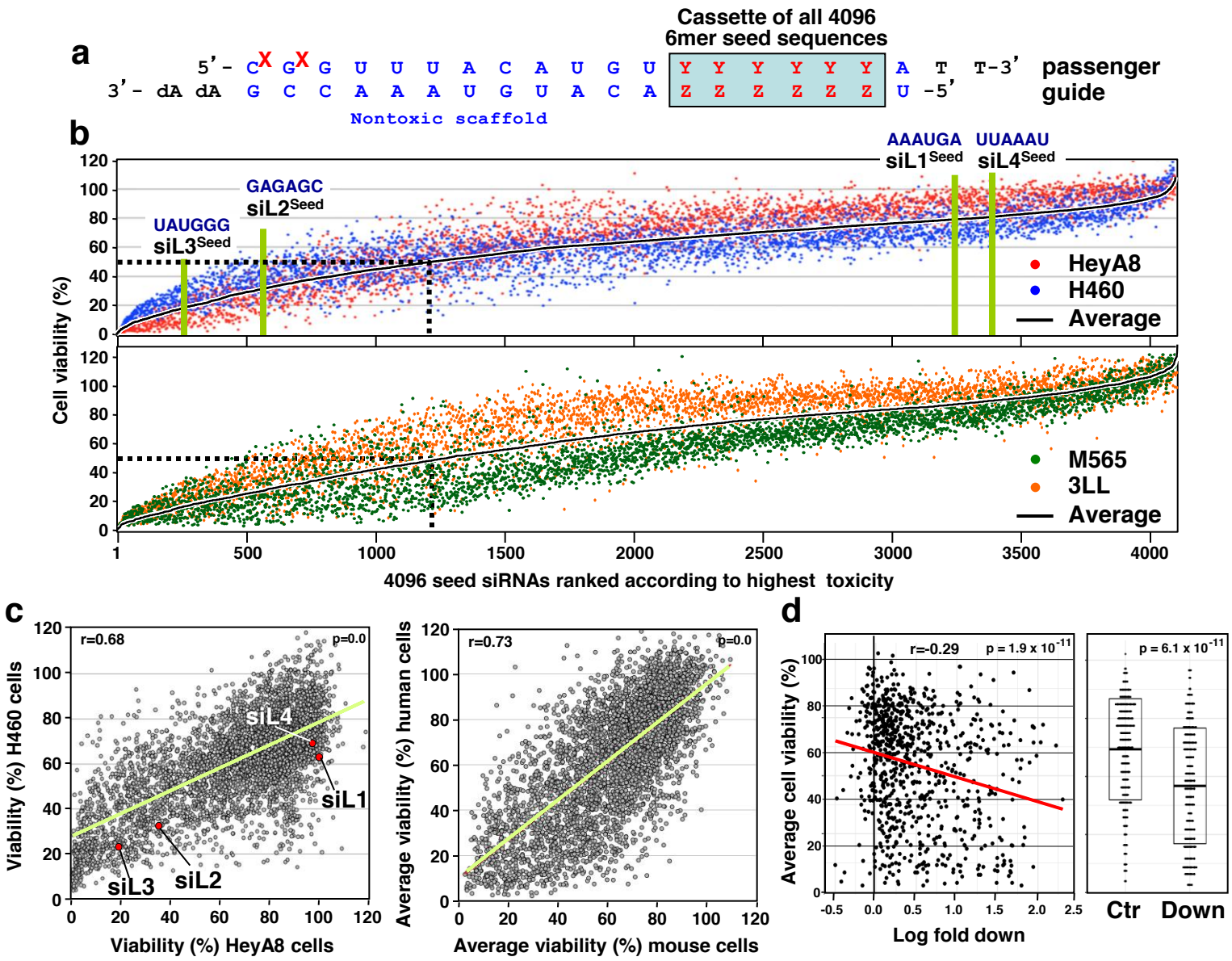
a
Cassette of all 4096
6mer seed sequences
5'- C X G X G U U U A C A U G U Y Y Y Y Y Y A T T-3' passenger
3'- dA dA G C C A A A U G U A C A Z Z Z Z Z Z U -5' guide
Nontoxic scaffold
b
AAAUGA siL1Seed
UUAAAU siL4Seed
GAGAGC siL2Seed
UAUGGG siL3Seed
HeyA8
H460
Average
M565
3LL
Average
Cell viability (%)
4096 seed siRNAs ranked according to highest toxicity
c
r=0.68
p=0.0
siL4
siL1
siL3
siL2
Viability (%) H460 cells
Viability (%) HeyA8 cells
r=0.73
p=0.0
Average viability (%) human cells
Average viability (%) mouse cells
d
r=-0.29
p = 1.9 x 10-11
Average cell viability (%)
Log fold down
p = 6.1 x 10-11
Ctr
Down

Figure 2

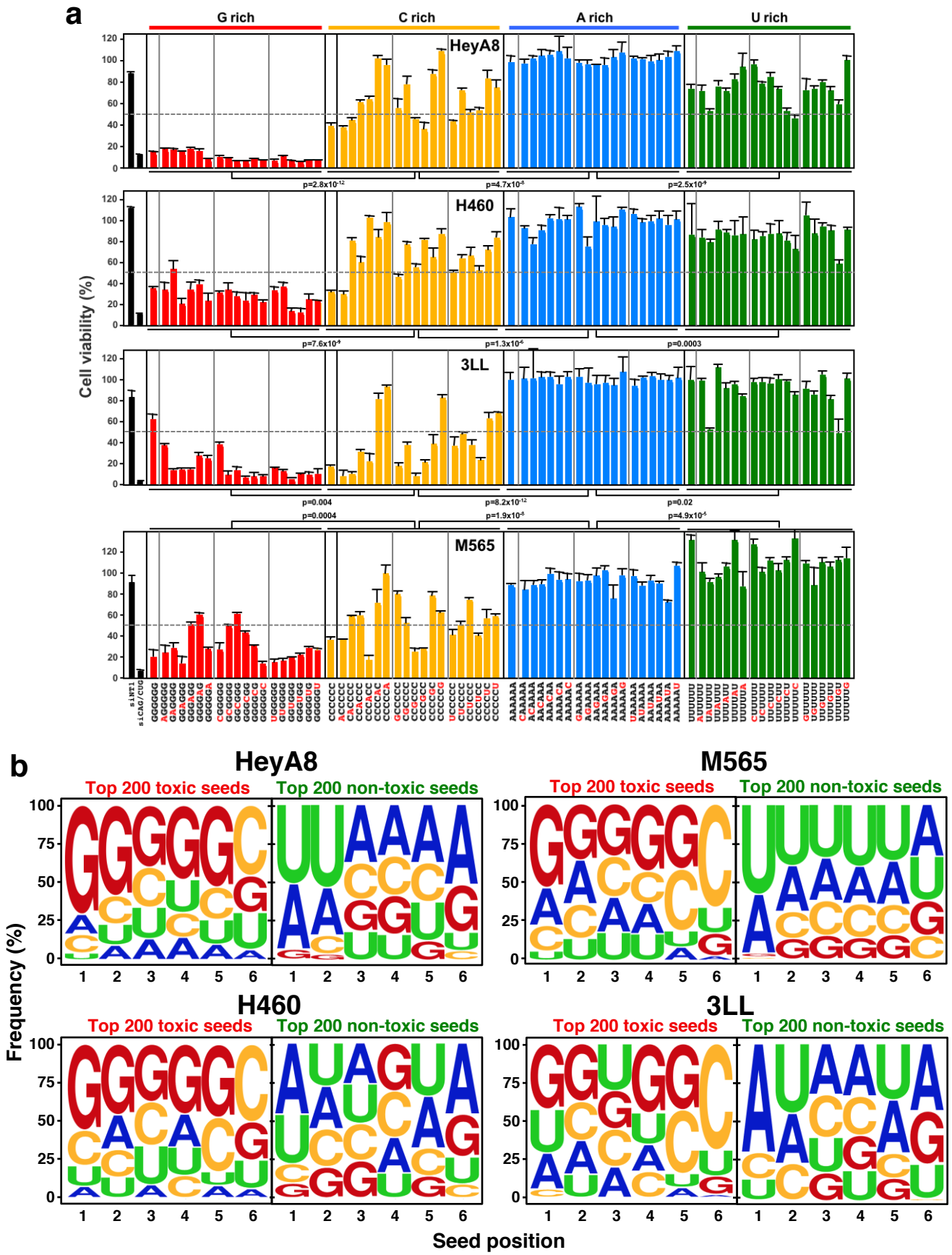
a
G rich
C rich
A rich
U rich
HeyA8
H460
3LL
M565
Cell viability (%)
p=2.8x10-12
p=4.7x10-8
p=2.5x10-9
p=7.6x10-9
p=1.3x10-6
p=0.0003
p=0.004
p=8.2x10-12
p=0.02
p=0.0004
p=1.9x10-8
p=4.9x10-5
siWT1
siCAG/CUG
b
HeyA8
M565
H460
3LL
Top 200 toxic seeds
Top 200 non-toxic seeds
Frequency (%)
Seed position

Figure 3

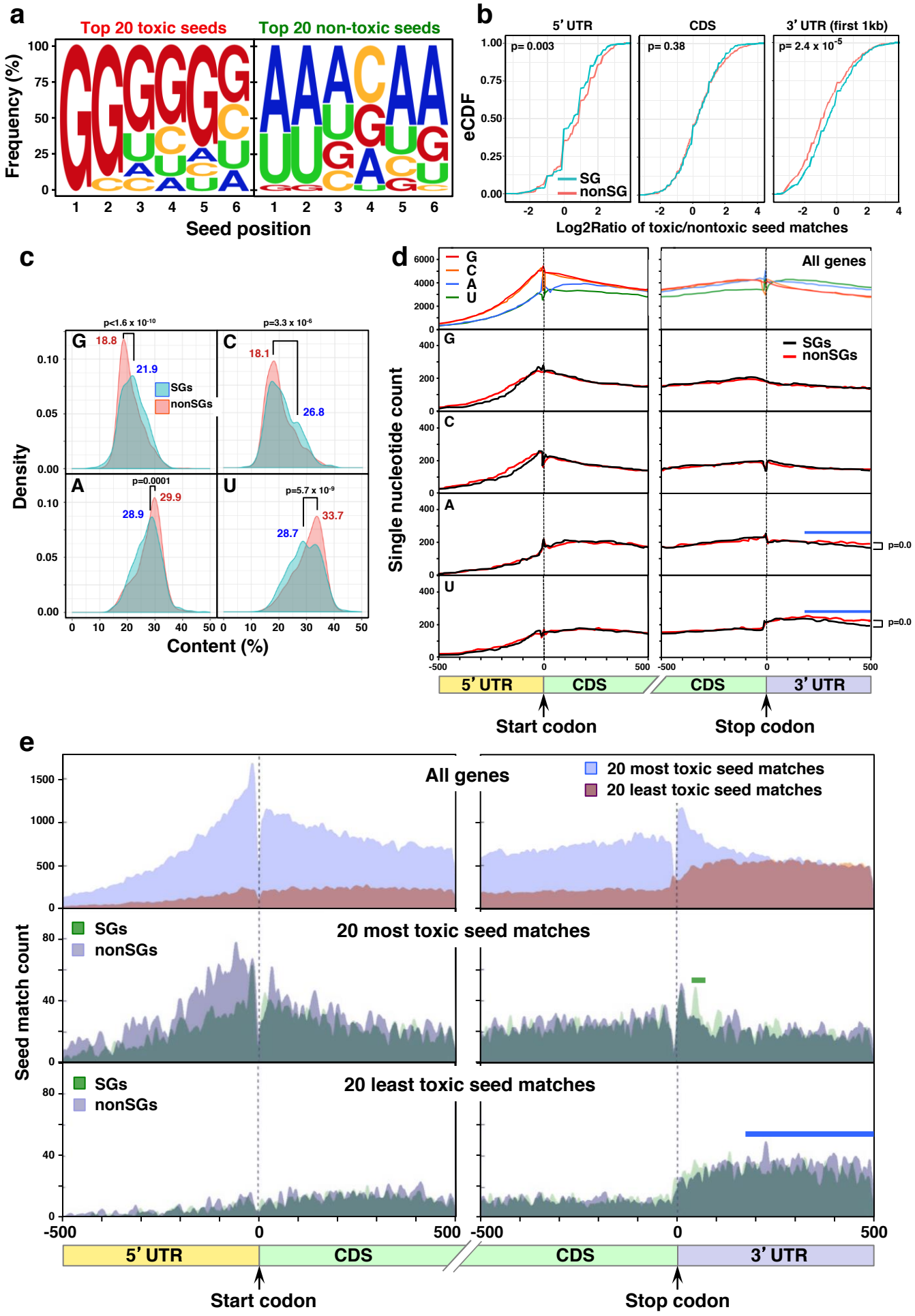
a
Top 20 toxic seeds
Top 20 non-toxic seeds
Frequency (%)
Seed position
b
5' UTR
CDS
3' UTR (first 1kb)
p= 0.003
p= 0.38
p= 2.4 x 10-5
eCDF
SG
nonSG
Log2Ratio of toxic/nontoxic seed matches
c
p<1.6 x 10-10
p=3.3 x 10-6
p=0.0001
p=5.7 x 10-9
18.8
21.9
18.1
26.8
28.9
29.9
28.7
33.7
SGs
nonSGs
Density
Content (%)
d
All genes
SGs
nonSGs
Single nucleotide count
5' UTR
CDS
3' UTR
Start codon
Stop codon
e
All genes
20 most toxic seed matches
20 least toxic seed matches
Seed match count
SGs
nonSGs
5' UTR
CDS
3' UTR
Start codon
Stop codon

Figure 4

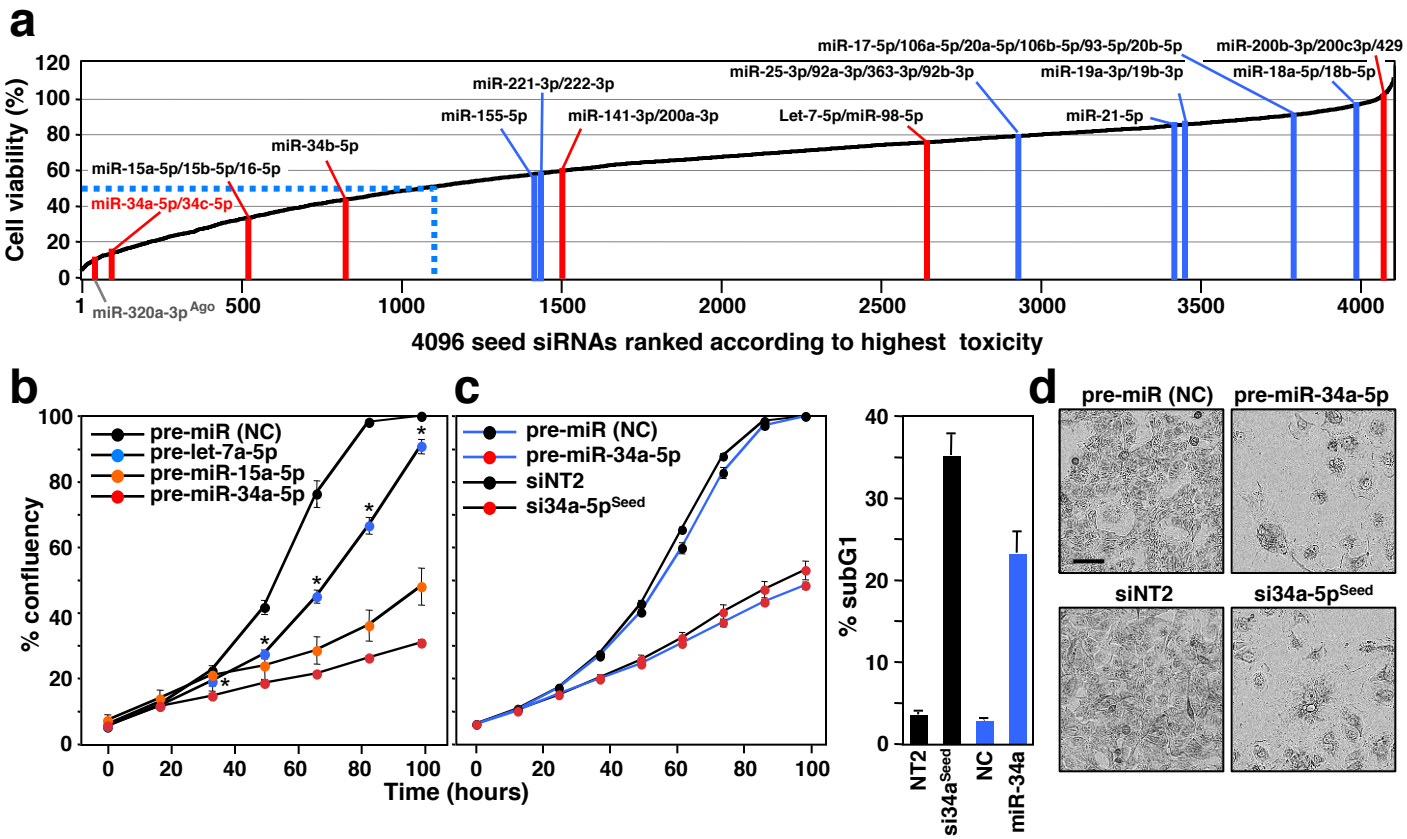
a
Cell viability (%)
miR-17-5p/106a-5p/20a-5p/106b-5p/93-5p/20b-5p
miR-200b-3p/200c3p/429
miR-25-3p/92a-3p/363-3p/92b-3p
miR-19a-3p/19b-3p
miR-18a-5p/18b-5p
miR-221-3p/222-3p
miR-155-5p
miR-141-3p/200a-3p
Let-7-5p/miR-98-5p
miR-21-5p
miR-34b-5p
miR-15a-5p/15b-5p/16-5p
miR-34a-5p/34c-5p
miR-320a-3p Ago
4096 seed siRNAs ranked according to highest toxicity
b
% confluency
pre-miR (NC)
pre-let-7a-5p
pre-miR-15a-5p
pre-miR-34a-5p
Time (hours)
c
pre-miR (NC)
pre-miR-34a-5p
siNT2
si34a-5pSeed
% subG1
NT2
si34aSeed
NC
miR-34a
d
pre-miR (NC)
pre-miR-34a-5p
siNT2
si34a-5pSeed

Figure 5

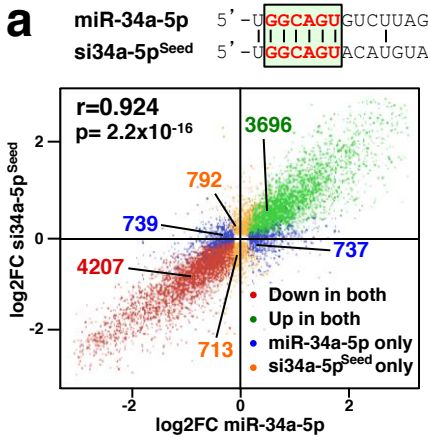

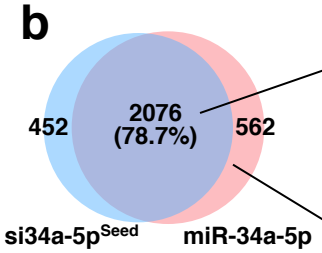

GO Term	Description	P-value	FDR q-value	Enrichment
GO:0022402	cell cycle process	3.25E-27	2.60E-23	2.0
GO:0065004	protein-DNA complex assembly	2.80E-23	1.12E-19	3.8
GO:0071824	protein-DNA complex subunit organization	6.06E-22	1.61E-18	3.6
GO:0006334	nucleosome assembly	3.38E-21	6.75E-18	3.9
GO:1903047	mitotic cell cycle process	8.37E-21	1.34E-17	2.0
GO:0034728	nucleosome organization	4.22E-20	5.62E-17	3.7
GO:0051276	chromosome organization	6.66E-19	7.59E-16	2.7
GO:0006325	chromatin organization	5.75E-16	5.74E-13	4.7
GO:0006342	chromatin silencing	5.37E-15	4.76E-12	4.3
GO:0045814	negative regulation of gene expression, epigenetic	1.16E-14	9.28E-12	4.1
GO:0016458	gene silencing	5.56E-13	4.03E-10	6.9
GO:0051301	cell division	7.46E-13	4.96E-10	2.0
GO:0038111	interleukin-7-mediated signaling pathway	1.64E-12	1.01E-09	19.3
GO:0000183	chromatin silencing at rDNA	3.29E-12	1.88E-09	5.3
GO:0006259	DNA metabolic process	4.15E-12	2.21E-09	1.5

GO Term	Description	P-value	FDR q-value	Enrichment
GO:0015718	monocarboxylic acid transport	4.59E-06	1.82E-02	22.5
GO:0006869	lipid transport	2.57E-05	5.09E-02	14.1
GO:0015850	organic hydroxy compound transport	1.02E-04	1.35E-01	22.5
GO:0015849	organic acid transport	1.83E-04	1.81E-01	6.0
GO:0046942	carboxylic acid transport	1.83E-04	1.45E-01	6.0
GO:0006820	anion transport	4.80E-04	3.17E-01	9.4

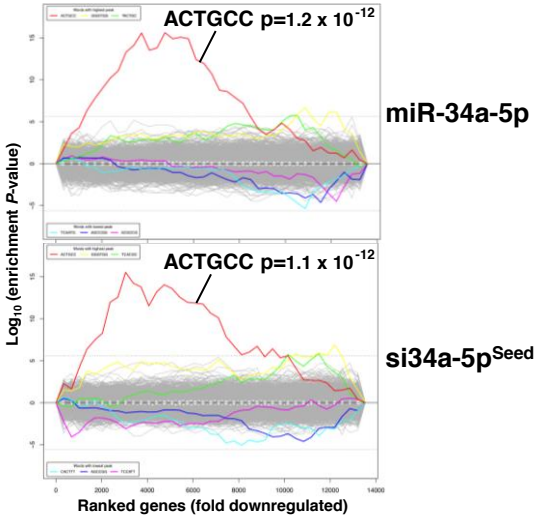

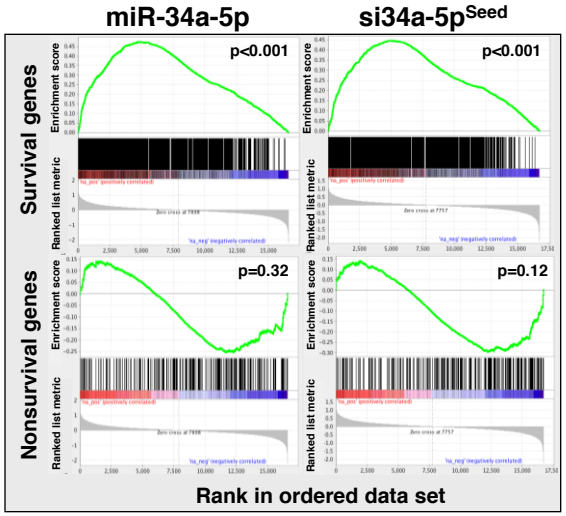

Figure 6

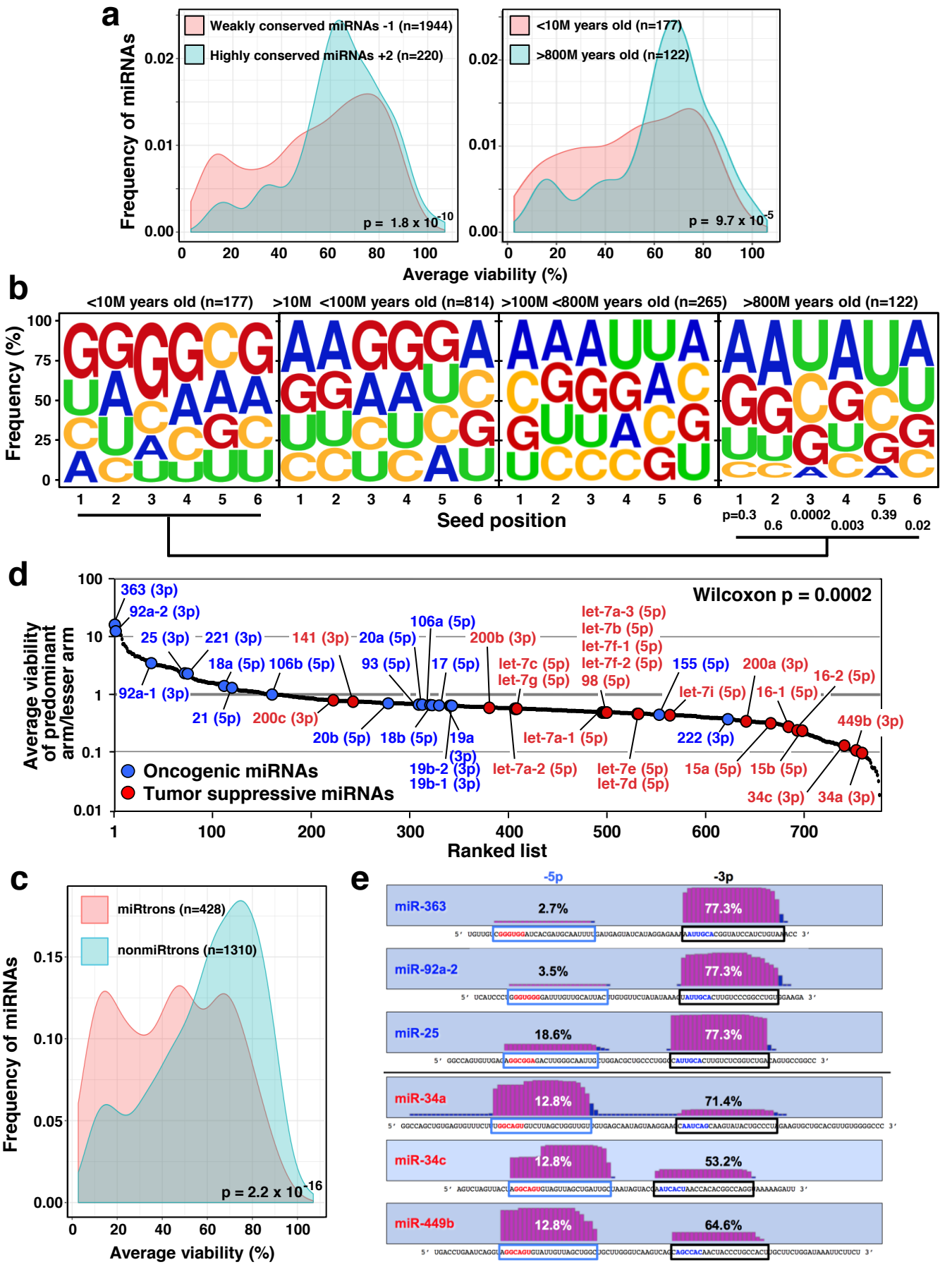
a
Weakly conserved miRNAs -1 (n=1944)
Highly conserved miRNAs +2 (n=220)
p = 1.8 x 10-10
<10M years old (n=177)
>800M years old (n=122)
p = 9.7 x 10-5
Frequency of miRNAs
Average viability (%)
b
<10M years old (n=177)
>10M <100M years old (n=814)
>100M <800M years old (n=265)
>800M years old (n=122)
Frequency (%)
Seed position
p=0.3
0.6
0.0002
0.003
0.39
0.02
d
Wilcoxon p = 0.0002
363 (3p)
92a-2 (3p)
25 (3p)
221 (3p)
141 (3p)
20a (5p)
106a (5p)
200b (3p)
let-7a-3 (5p)
let-7b (5p)
let-7f-1 (5p)
let-7f-2 (5p)
98 (5p)
155 (5p)
200a (3p)
16-2 (5p)
16-1 (5p)
449b (3p)
18a (5p)
106b (5p)
93 (5p)
17 (5p)
let-7c (5p)
let-7g (5p)
let-7i (5p)
92a-1 (3p)
21 (5p)
200c (3p)
20b (5p)
18b (5p)
19a (3p)
let-7a-1 (5p)
222 (3p)
19b-2 (3p)
19b-1 (3p)
let-7a-2 (5p)
let-7e (5p)
let-7d (5p)
15a (5p)
15b (5p)
34c (3p)
34a (3p)
Oncogenic miRNAs
Tumor suppressive miRNAs
Average viability of predominant arm/lesser arm
Ranked list
c
miRtrons (n=428)
nonmiRtrons (n=1310)
p = 2.2 x 10-16
Frequency of miRNAs
Average viability (%)
e
-5p
-3p
miR-363
2.7%
77.3%
miR-92a-2
3.5%
77.3%
miR-25
18.6%
77.3%
miR-34a
12.8%
71.4%
miR-34c
12.8%
53.2%
miR-449b
12.8%
64.6%

Figure 7

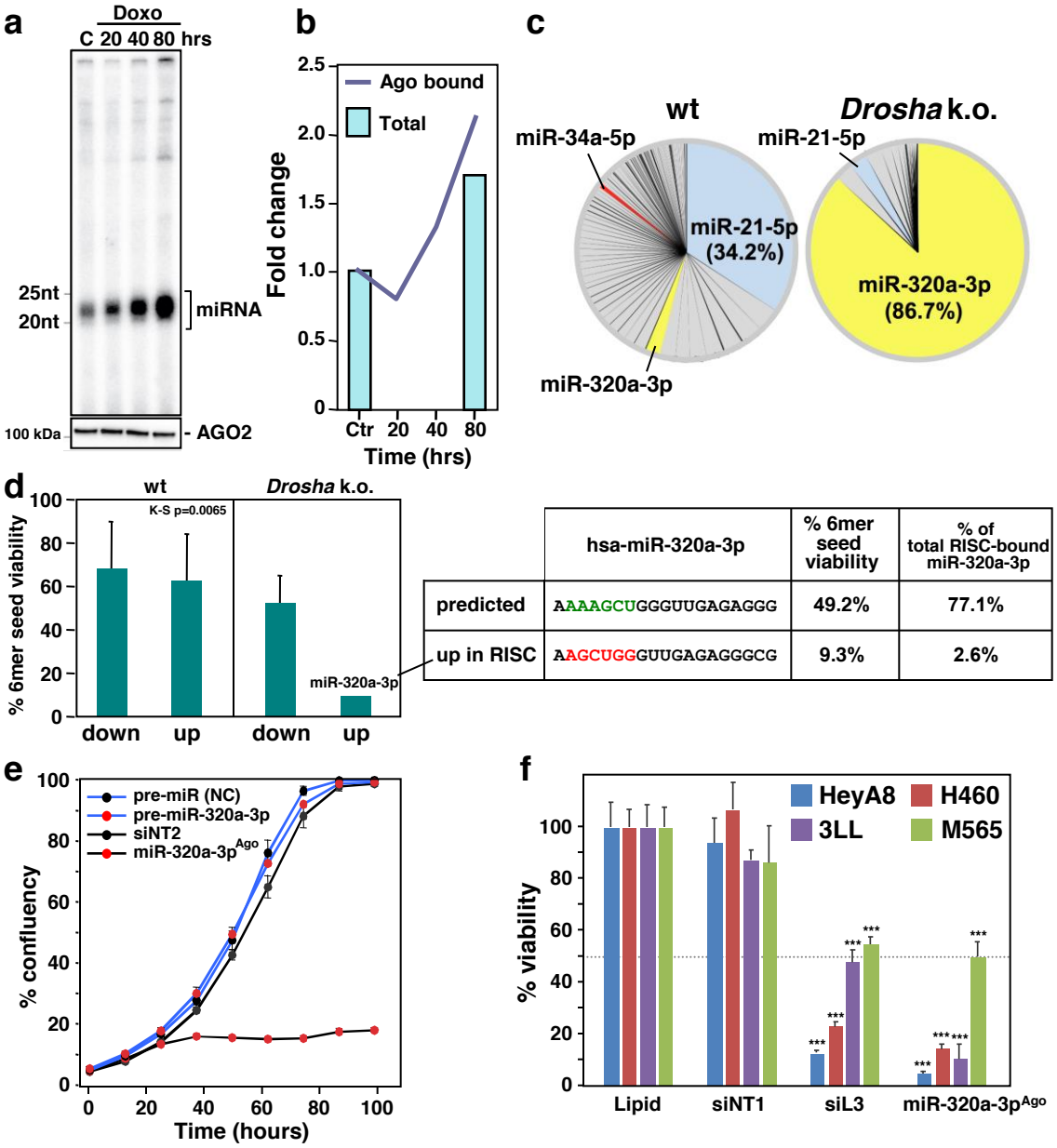

	hsa-miR-320a-3p	% 6mer seed viability	% of total RISC-bound miR-320a-3p
predicted	AAAAGCUGGGUUGAGAGGG	49.2%	77.1%
up in RISC	AAGCUGGGUUGAGAGGGCG	9.3%	2.6%